Maryland Mainstem Tributary Summary:

A summary of trends in tidal water quality and associated factors, 1985-2018.

June 7, 2021

Prepared for the Chesapeake Bay Program (CBP) Partnership by the CBP Integrated Trends Analysis Team (ITAT)

Chesapeake Bay Program
Science. Restoration. Partnership.

This tributary summary is a living document in draft form and has not gone through a formal peer review process. We are grateful for contributions to the development of these materials from the following individuals: Jeni Keisman, Rebecca Murphy, Olivia Devereux, Jimmy Webber, Qian Zhang, Meghan Petenbrink, Tom Butler, Zhaoying Wei, Jon Harcum, Renee Karrh, Mike Lane, and Elgin Perry.

Contents

1. Purpose and Scope

The Maryland Mainstem Summary outlines change over time in a suite of monitored tidal water quality parameters and associated potential drivers of those trends for the time period 1985 – 2018 and provides a brief description of the current state of knowledge explaining these observed changes. Water quality parameters described include surface (above pycnocline) total nitrogen (TN), surface total phosphorus (TP), spring and summer surface chlorophyll *a*, summer bottom (below pycnocline) dissolved oxygen (DO) concentrations, and Secchi disk depth (a measure of water clarity). Results for annual surface water temperature, bottom TP, bottom TN, surface ortho-phosphate (PO4), surface dissolved inorganic nitrogen (DIN), surface total suspended solids (TSS), and summer surface DO concentrations are provided in an Appendix. Drivers discussed include physiographic watershed characteristics, changes in TN, TP, and sediment loads from the watershed to tidal waters, expected effects of changing land use, and implementation of nutrient management and natural resource conservation practices. Factors internal to estuarine waters that also play a role as drivers are described including biogeochemical processes, physical forces such as wind-driven mixing of the water column, and biological factors such as phytoplankton biomass and the presence of submerged aquatic vegetation. Continuing to track water quality response and investigating these influencing factors are important steps to understanding water quality patterns and changes in the Maryland Mainstem.

2. Location

For the purposes of this summary, the Maryland Mainstem is defined as that portion of the Bay extending from the mouth of the Maryland Mainstem past the Choptank and Little Choptank Rivers on the eastern shore, to end just above the mouth of the western shore's Patuxent River. Its watershed is dominated by the Maryland Mainstem drainage basin, while also receiving contributions from areas along the upper eastern and western shorelines. The Maryland Mainstem watershed covers approximately 43.8% of the Chesapeake Bay Watershed. Its watershed is approximately 71967 km2 (Table 1.) and is contained within three states, New York, Pennsylvania, and Maryland (Figure 1).

Tributary Name	Watershed Area km2
MARYLAND MAINSTEM	71967
POTOMAC	36611
JAMES	25831
YORK	6537
RAPPAHANNOCK	6530
LOWER EASTERN SHORE	4532
MARYLAND UPPER EASTERN SHORE	2441
PATUXENT	2236
VIRGINIA MAINSTEM	2052
CHOPTANK	1844
PATAPSCO-BACK	1647
MARYLAND UPPER WESTERN SHORE	1523
MARYLAND LOWER WESTERN SHORE	439

Table 1. "Watershed areas for each of the thirteen tributary or tributary groups for which Tributary Trends summaries have been produced. All of the tributary summaries can be accessed at the following link: https://cast.chesapeakebay.net/Home/TMDLTracking#tributaryRptsSection".

2.1 Watershed Physiography

The Maryland Mainstem's watershed stretches across five major physiographic regions, namely, Valley and Ridge, Piedmont, Coastal Plain, Blue Ridge, and Mesozoic Lowland (Bachman *et al.*, 1998) (Figure 1). The Valley and Ridge physiography covers both carbonate and siliciclastic areas. The Piedmont physiography covers both carbonate and crystalline areas. The Coastal Plain physiography covers lowland, dissected upland, and upland areas. Implications of this physiography for nutrient and sediment transport are summarized in Section 5.1.1.

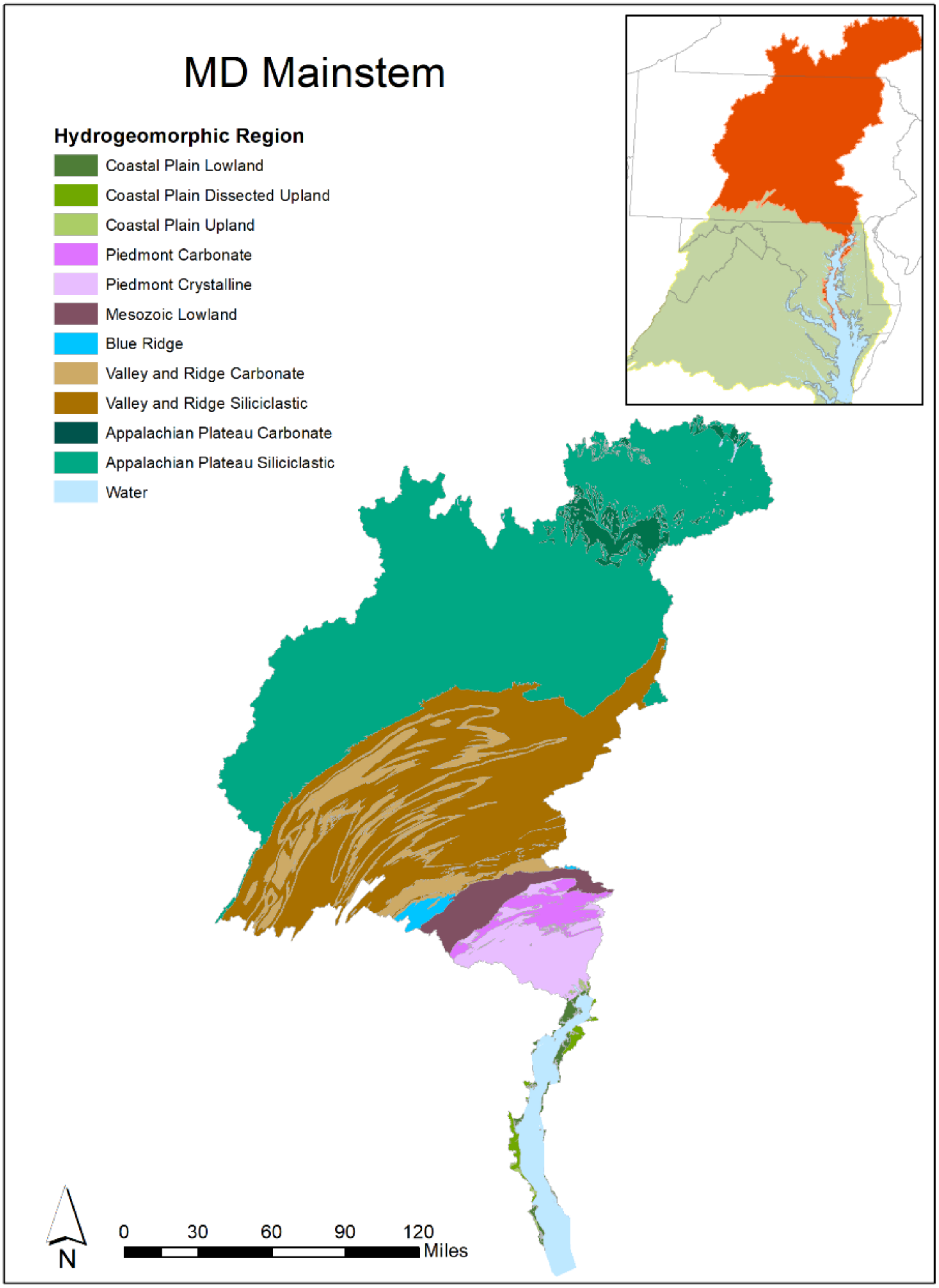

Figure 1. Distribution of physiography in the Maryland Mainstem watershed.

2.2 Land Use

Land use in the Maryland Mainstem watershed is dominated (68%) by natural areas. Urban and suburban land areas have increased by 532,999 acres since 1985, agricultural lands have decreased by 664,644 acres, and natural lands have increased by 129,998 acres. Correspondingly, the proportion of urban land in this watershed has increased from 8% in 1985 to 11% in 2019 (Figure 2).

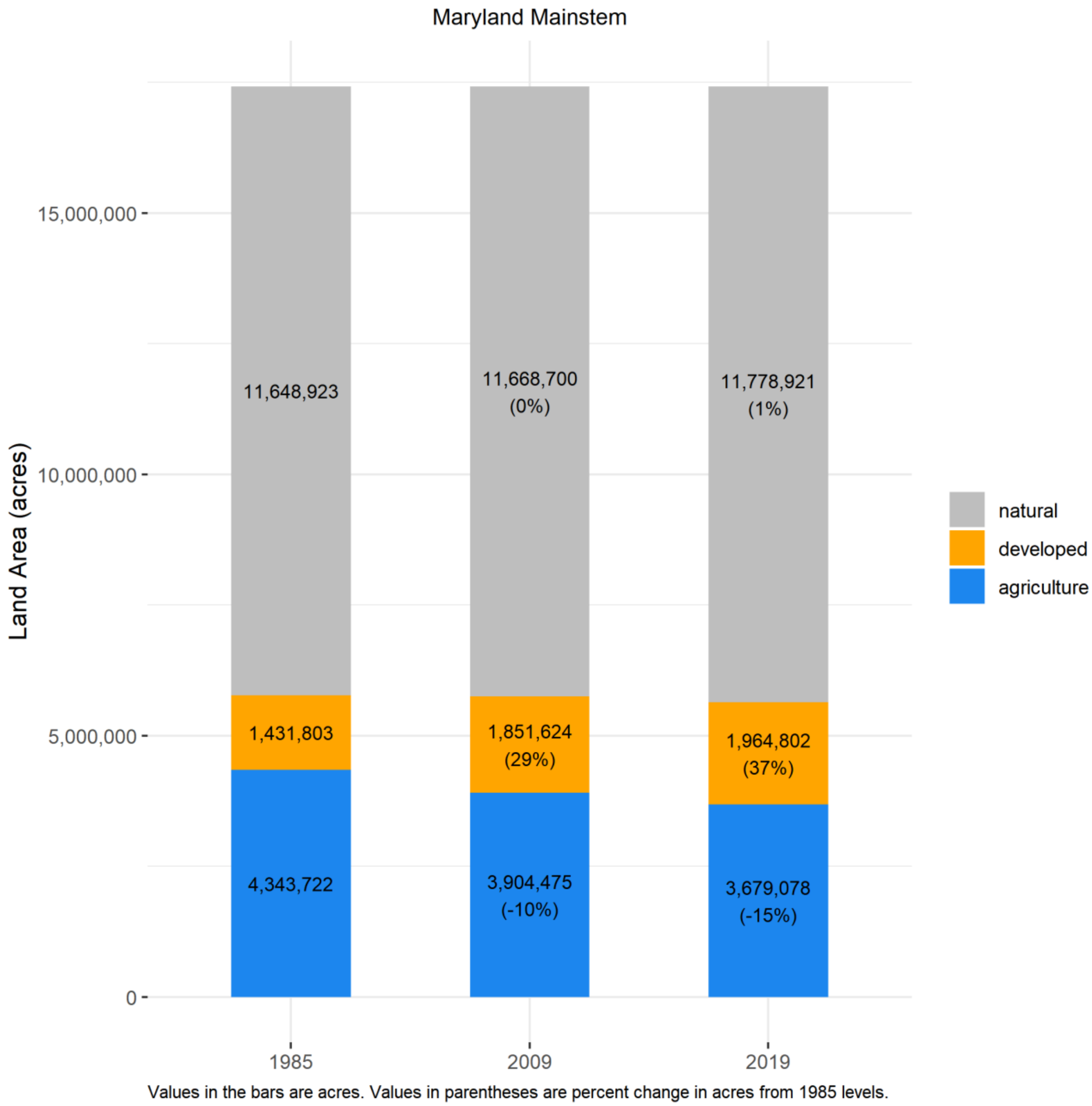

Figure 2. Distribution of land uses in the Maryland Mainstem watershed. Percentages are the percent change from 1985 for each source sector.

In general, developed lands in the 1970s were more concentrated within towns and major metropolitan areas. Since then, developed and semi-developed lands have expanded around these areas, as well as extending into previously undeveloped regions (Figure 3). The impacts of land development differ depending on the use from which the land is converted (Keisman *et al.*, 2019; Ator *et al.*, 2019). Implications of changing land use for nutrient and sediment transport are summarized in Section 5.1.3.

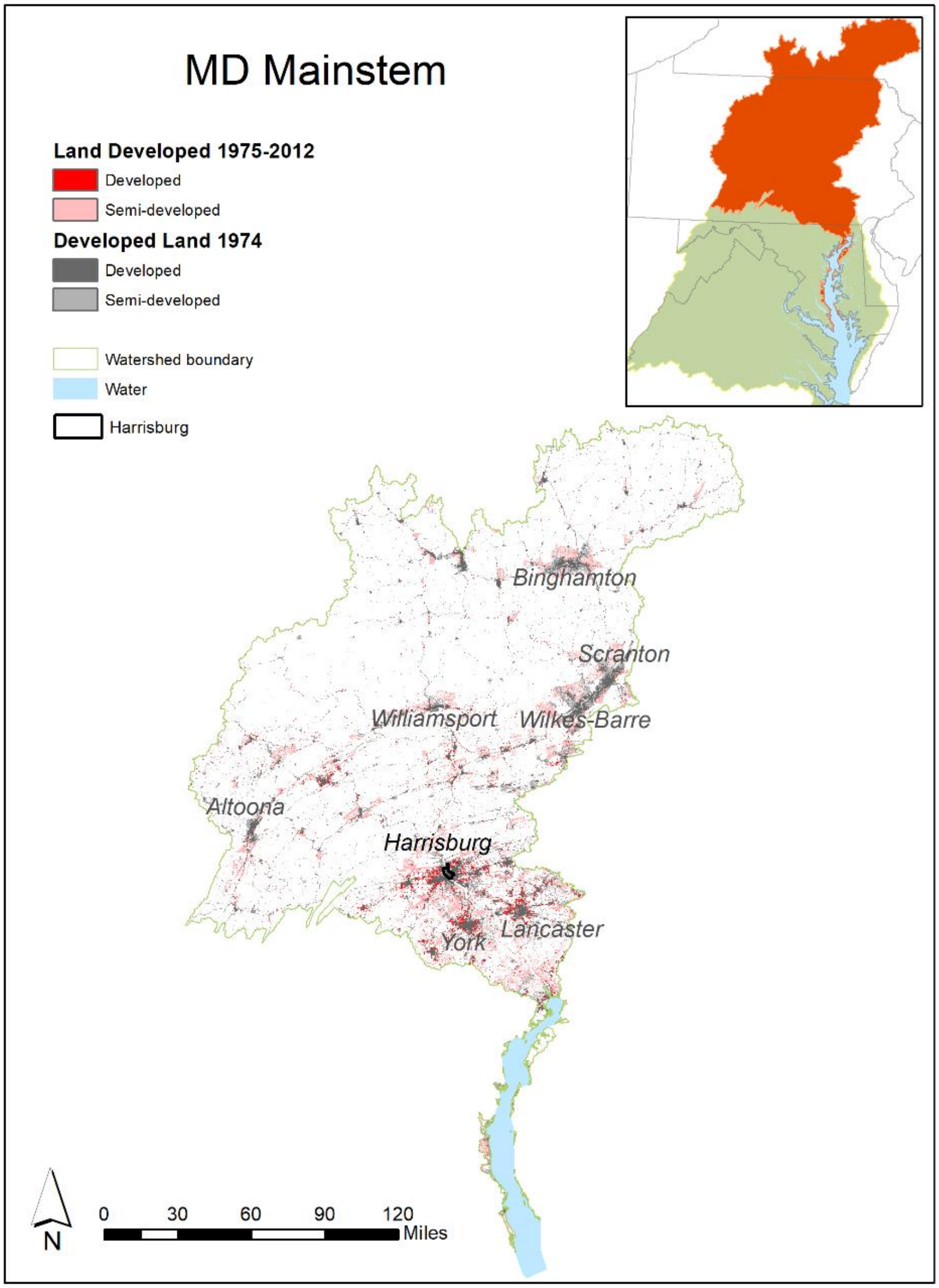

Figure 3. Distribution of developed land in the Maryland Mainstem watershed. Derived from Falcone (2015). Base map credit Chesapeake Bay Program, www.chesapeakebay.net, North American Datum 1983.

2.3 Tidal Waters and Stations

For the purposes of water quality standards assessment and reporting, the Upper Chesapeake is divided into five segments (U.S. Environmental Protection Agency, 2004): the northernmost Tidal Fresh region (CB1TF), the Oligohaline region of the Upper Chesapeake (CB2OH), and three Mesohaline regions (CB3MH, CB4MH, and CB5MH_MD) (Figure 4).

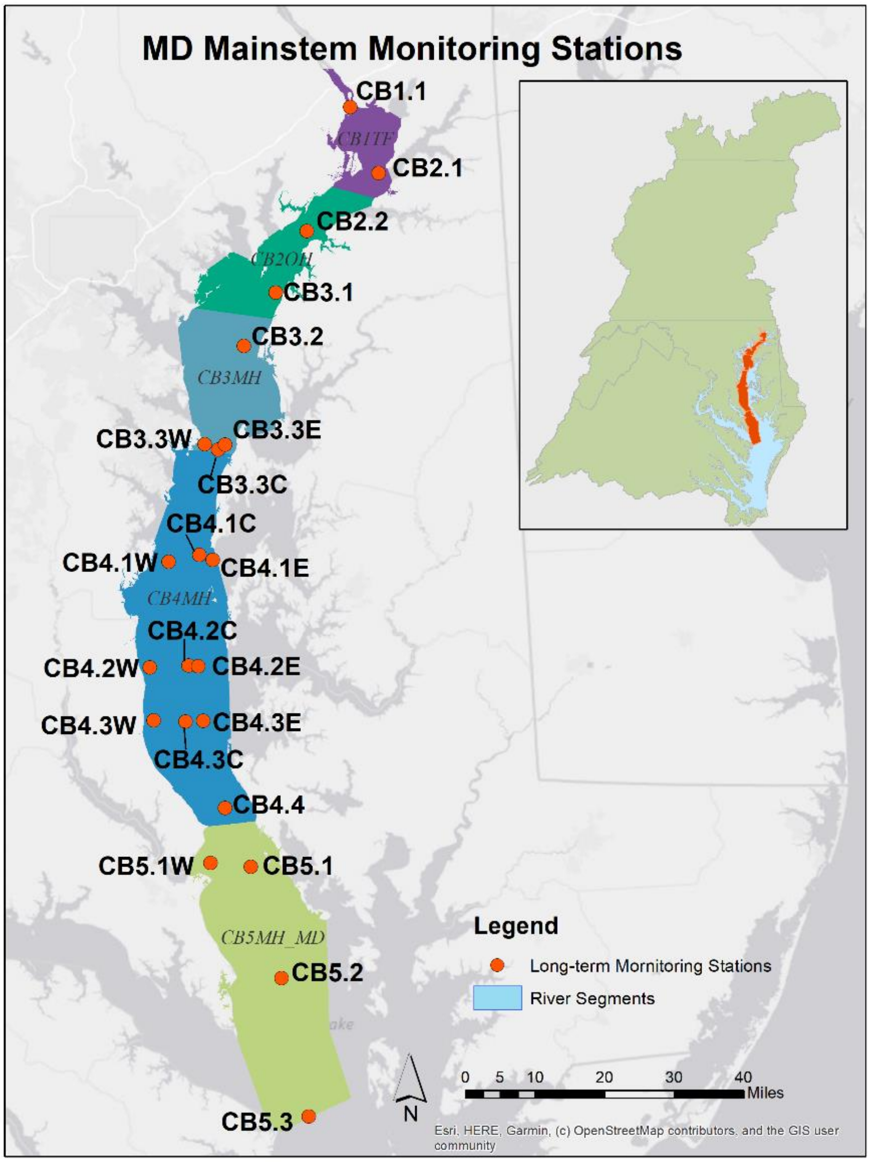

Figure 4. Map of Maryland Mainstem segments and long-term monitoring stations. Base map credit Esri, HERE, Garmin, (c) OpenStreetMap contributors, and the GIS user community, World Geodetic System 1984.

Long-term trends in water quality are analyzed by MD Department of Natural Resources at 22 stations stretching from the mouth of the Maryland Mainstem River to the Virginia state line (Figure 4). Water quality data at these stations are also used to assess attainment of dissolved oxygen (DO) water quality criteria. All tidal water quality data analyzed for this summary are available from the Chesapeake Bay Program Data Hub (Chesapeake Bay Program, 2018). Other monitoring has been conducted over the years and used for water quality criteria evaluation but is not shown in the long-term trend graphics in subsequent sections because of its shorter duration.

3. Tidal Water Quality Dissolved Oxygen Criteria Attainment

Multiple water quality standards were developed for Chesapeake Bay to protect aquatic living resources (U.S. Environmental Protection Agency, 2003; Tango and Batiuk, 2013). These standards include specific criteria for dissolved oxygen (DO) and water clarity/underwater bay grasses. For the purposes of this summary, a record of the evaluation results indicating whether each of the MD mainstem segments have met or not met a 30 day or instantaneous of Open Water (OW), Deep Water (DW), and Deep Channel (DC) DO criteria over time is shown below (Zhang *et al.*, 2018a; Hernandez Cordero *et al.*, 2020). While analysis of water quality standards attainment is not the focus of this summary, the results (Tables 2 and 3) provide context for the importance of understanding factors affecting water quality trends. For more information on water quality standards, criteria, and standards attainment, visit the CBP's "Chesapeake Progress" website at www.chesapeakeprogress.com. In the recent period (2016-2018), three of the five MD mainstem segments met the 30-day mean OW summer DO requirements, while none of the segments with DW or DC requirements met them (Zhang *et al.*, 2018b).

Table 2. Open Water summer DO criterion evaluation results (30-day mean June-September assessment period). Green indicates that the criterion was met. White indicates that the criterion was not met.

Time Period	CB1TF	CB2OH	CB3MH	CB4MH	CB5MH_MD
1985-1987					
1986-1988					
1987-1989					
1988-1990					
1989-1991					
1990-1992					
1991-1993					
1992-1994					
1993-1995					
1994-1996					
1995-1997					
1996-1998					
1997-1999					
1998-2000					
1999-2001					
2000-2002					
2001-2003					
2002-2004					
2003-2005					

2004-2006					
2005-2007					
2006-2008					
2007-2009					
2008-2010					
2009-2011					
2010-2012					
2011-2013					
2012-2014					
2013-2015					
2014-2016					
2015-2017					
2016-2018					

Table 3. Deep Water summer DO (30-day mean) and Deep Channel (Instantaneous) DO criteria evaluation results. Green indicates that the criterion was met. White indicates that the criterion was not met. (Note: the entire table is white intentionally because these criteria have not been met during this period.)

Time Period	Deep Water			Deep Channel		
	CB3MH	CB4MH	CB5MH_MD	CB3MH	CB4MH	CB5MH_MD
1985-1987						
1986-1988						
1987-1989						
1988-1990						
1989-1991						
1990-1992						
1991-1993						
1992-1994						
1993-1995						
1994-1996						
1995-1997						
1996-1998						
1997-1999						
1998-2000						
1999-2001						
2000-2002						
2001-2003						
2002-2004						
2003-2005						
2004-2006						
2005-2007						
2006-2008						
2007-2009						
2008-2010						
2009-2011						
2010-2012						
2011-2013						
2012-2014						
2013-2015						

2014-2016						
2015-2017						
2016-2018						

Comparing trends in station-level DO concentrations to the computed DO criterion status for a recent assessment period can reveal valuable information, such as whether progress is being made towards attainment in a segment that is not meeting the water quality criteria, or conversely the possibility that conditions are degrading even if the criteria are currently being met. To illustrate this, the 2016-2018 attainment status for the OW summer and DC instantaneous DO criteria shown in Tables 2 and 3 are overlain with the 1985-2018 change in summer surface DO concentration and the 1985-2018 change in bottom summer DO concentrations, respectively (Figure 5). Notably the DO concentrations both in the surface and the bottom are improving at many of the stations, suggesting progress even in regions not meeting water quality criteria. Improvements in surface concentrations are occurring in the two segments not meeting the 30-day mean OW summer DO criterion. Concentrations are possibly improving at almost all the bottom stations throughout the three segments not meeting the applicable DC criterion.

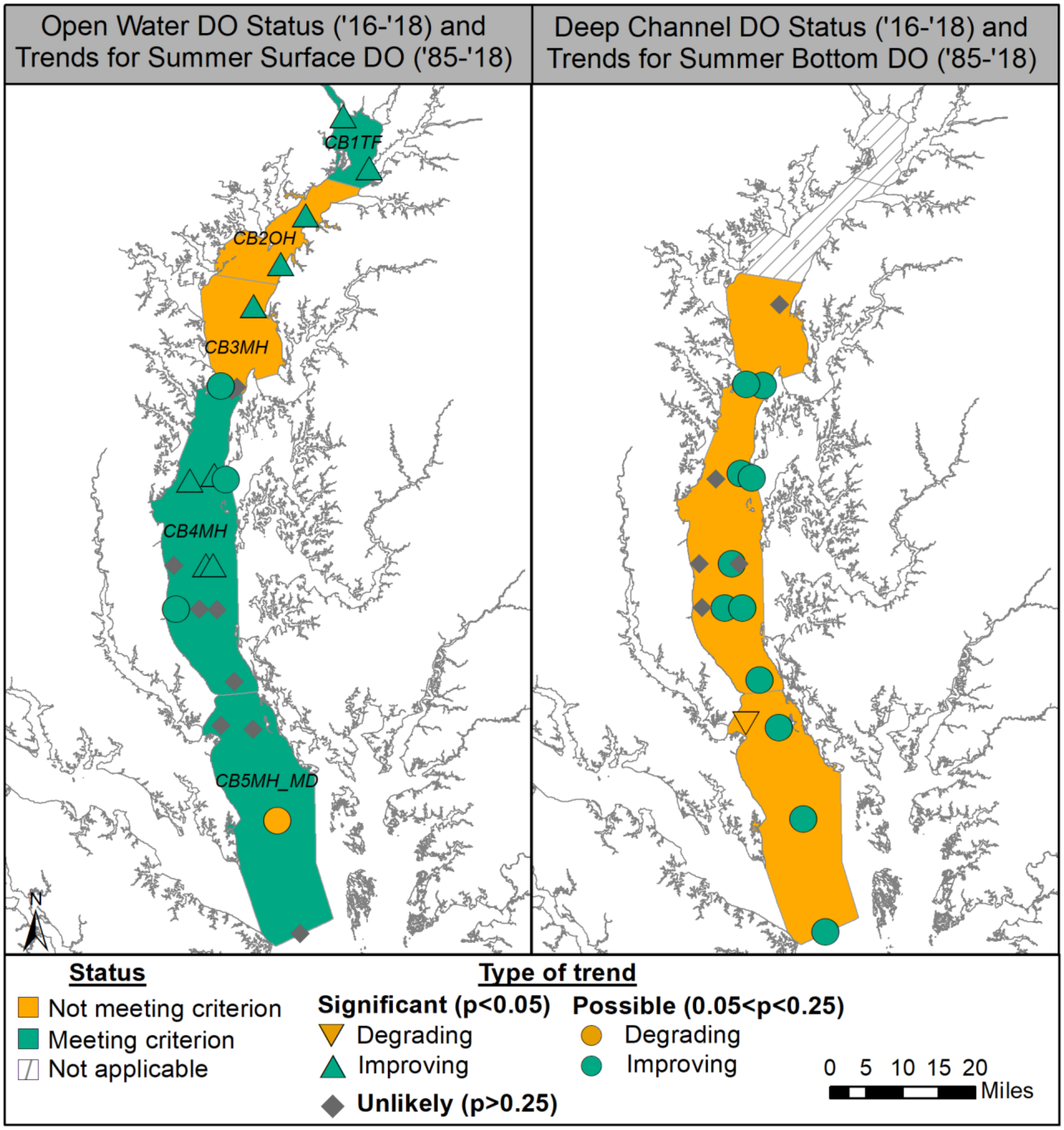

Figure 5. Pass-fail DO criterion status for 30-day OW summer DO and DC summer DO designated uses in MD mainstem segments along with long-term trends in DO concentrations. Base map credit Chesapeake Bay Program, www.chesapeakebay.net, North American Datum 1983.

4. Tidal Water Quality Trends

Tidal water quality trends are computed by fitting generalized additive models (GAMs) to the water quality observations that have been collected since the 1980s at the 22 stations labeled in Figure 4. Samples have been collected one or two times per month every year at 14 of these stations, allowing for estimates of annual change over time. The other eight stations have consistent samples in spring and summer seasons only, so only seasonal results are shown for those stations. For more details on the GAM implementation that is applied each year by MD Department of Natural Resources for these mainstem Chesapeake Bay stations in collaboration with the Chesapeake Bay Program and Virginia analysts, see Murphy *et al.* (2019).

Results shown below in each set of maps (e.g., Figure 6) include those generated using two different GAM fits to each station-parameter combination. The first approach involves fitting a GAM to the raw observations to generate a mean estimate of the concentrations over time, as observed in the estuary. The second approach involves including monitored river flow or *in situ* salinity (as an aggregated measure of multiple river flows) in the GAM to explain some of the variation in the water quality parameter. From the results of this second approach, it is possible to estimate the "flow-adjusted" change over time, which gives a mean estimate of what the water quality parameter trend would have been if river flow had been average over the period of record. Note that depending on station and parameter, sometimes gaged river flow is used for this adjustment and sometimes salinity is used, but we refer to all these results as "flow-adjusted" for simplicity.

To determine if there has been a change over time (i.e., a trend) at a particular station for a given parameter, we compute a percent change between the estimates at beginning and end of a period of interest from the GAM fit. For each percent change computation, the level of statistical confidence can be computed as well. Change is called significant if $p < 0.05$ and possible if the p-value is up to 0.25. That upper limit is higher than usually reported for hypothesis tests but allows us to provide a more complete picture of the results, identifying locations where change might be starting to occur and should be investigated (Murphy *et al.*, 2019). In addition to the maps of trends, for each parameter, there is a set of graphs (e.g., Figure 7) that include the raw observations (dots on the graphs) and lines representing the mean annual or seasonal GAM estimates, without flow-adjustment. The flow-adjusted GAM line graphs are not shown. For the eight mainstem MD stations sampled only in the spring and summer, trend results and GAM graphics are only shown for parameters with seasonal results (summer bottom oxygen, spring and summer chlorophyll *a*).

4.1 Surface Total Nitrogen

Annual total nitrogen (TN) trends vary at the MD mainstem stations (Figure 6). The upper half of the stations have degrading or no long-term TN trends without flow-adjustment. These same stations are improving or have no trend over the long-term with flow-adjustment. The lower half of the stations are improving over the long-term, with and without flow-adjustment. Over the short-term, there are more degrading trends with both approaches (Figure 6).

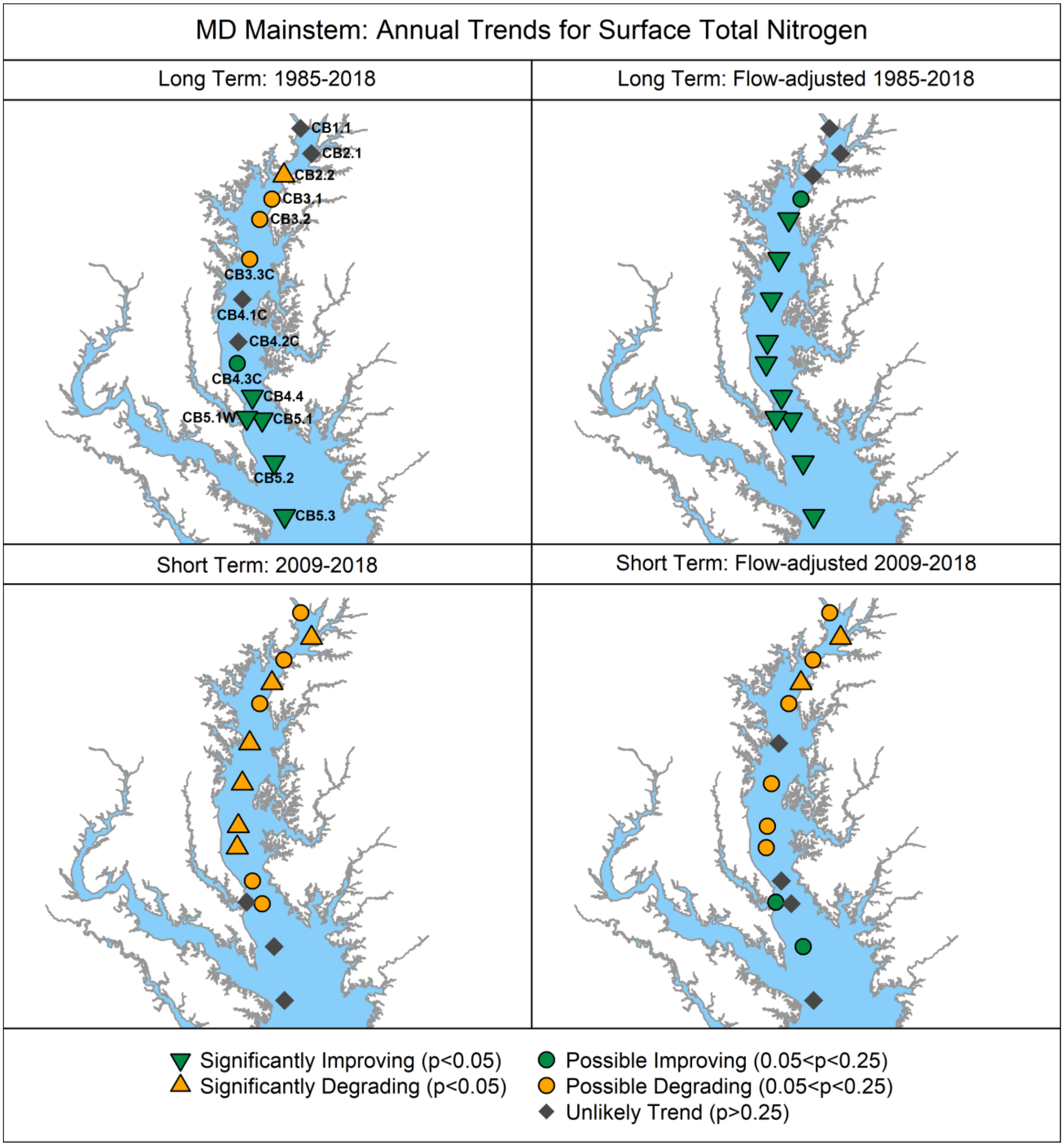

Figure 6. Surface TN trends. Base map credit Chesapeake Bay Program, www.chesapeakebay.net, North American Datum 1983.

The TN data and non-flow-adjusted mean annual GAM estimates at these stations all show an upswing in the last years of this record (Figure 7). Those larger concentrations resulted in the short-term degrading trends as well as some of the long-term degradations presented in Figure 6. Gradual long-term decreases are occurring at the CB4MH and CB5MH_MD stations (Figure 7).

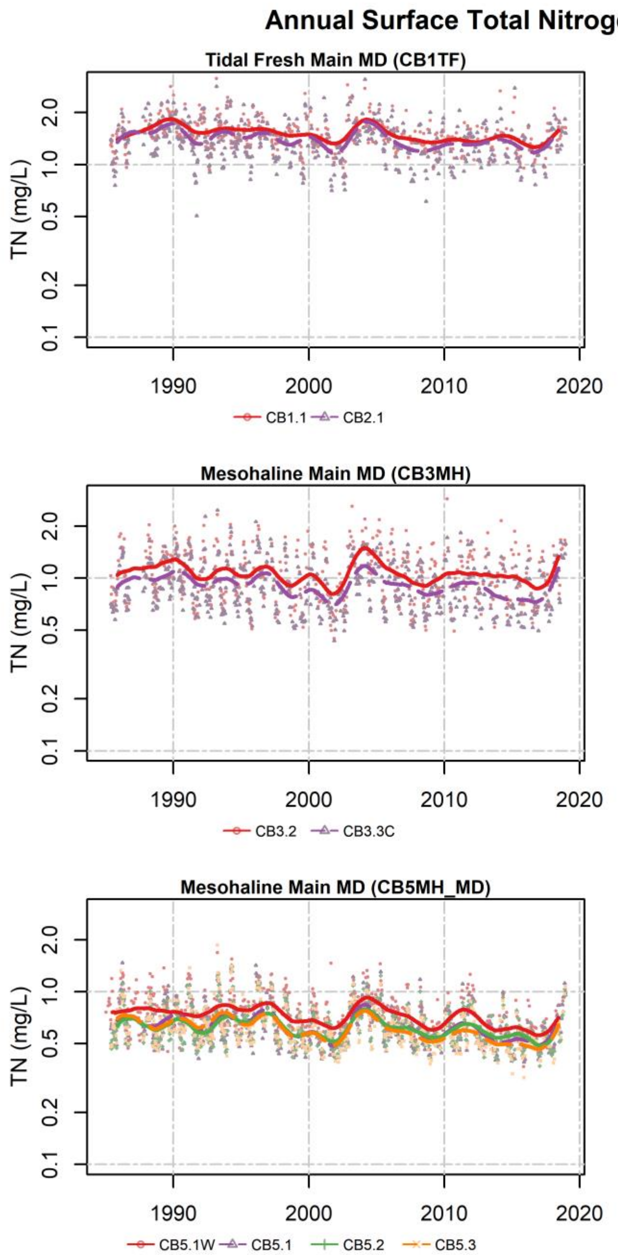

Figure 7. Surface TN data (dots) and average long-term pattern generated from non-flow-adjusted GAMs. Colored dots represent data corresponding to the monitoring station indicated in the legend; colored lines represent mean annual GAM estimates for the noted monitoring stations.

4.2 Surface Total Phosphorus

Surface total phosphorus (TP) is improving at almost all of the upper bay stations from CB1.1 to CB3.2, with and without flow-adjustment over the long- and short-term (Figure 8). Another group of stations, CB4.2C to CB5.2, are generally degrading over the long-term while over the short-term they are either showing no trend (not-adjusted) or improving (flow-adjusted). In addition, CB5.1W stands out as having improving trends in most cases (Figure 8).

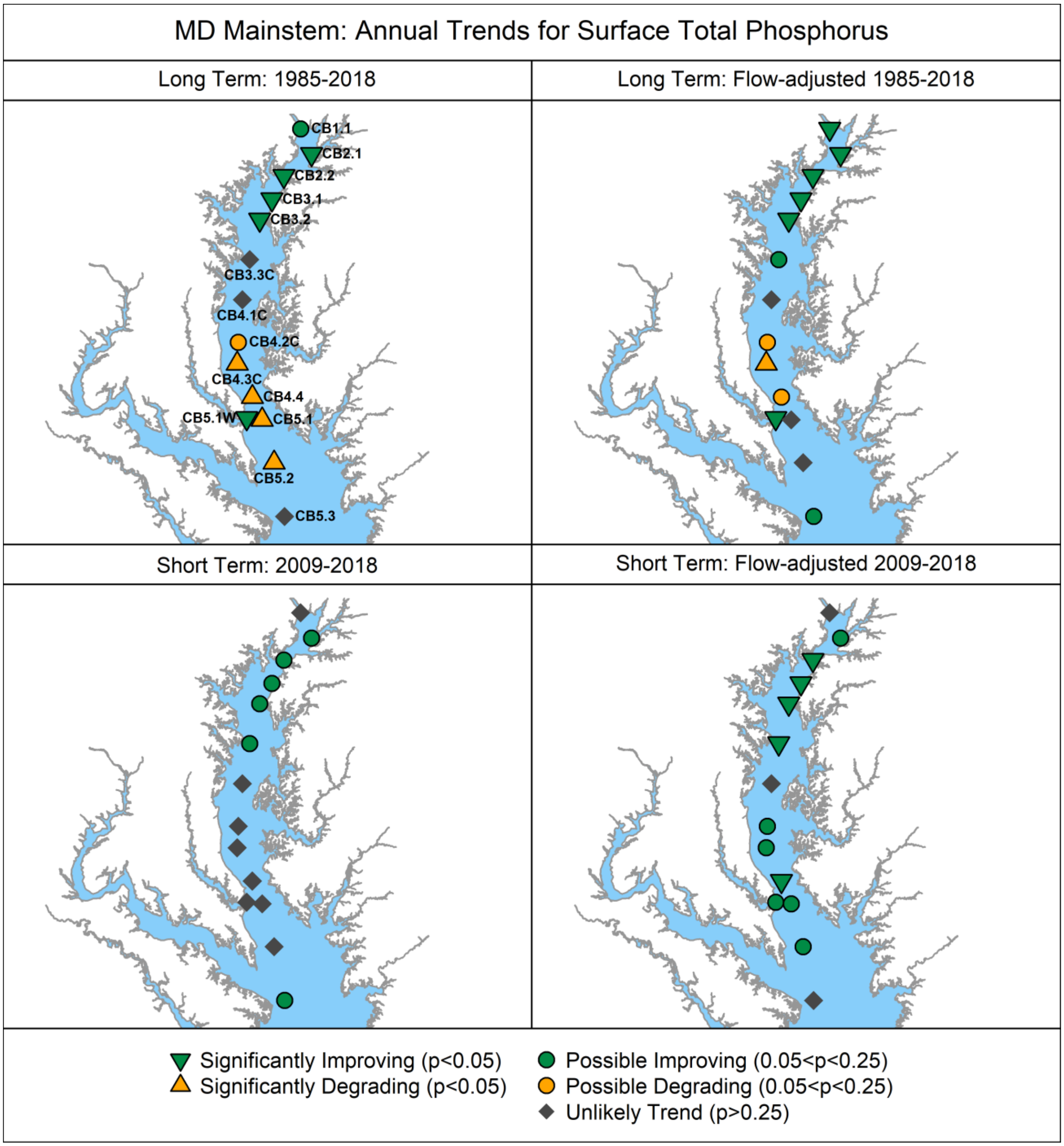

Figure 8. Surface TP trends. Base map credit Chesapeake Bay Program, www.chesapeakebay.net, North American Datum 1983.

The long-term decreases at the tidal fresh stations are clear from the data and mean annual GAM estimates (Figure 9). Decreases at the oligohaline stations are less obvious, although there has been a decrease from the beginning to the end of the record.

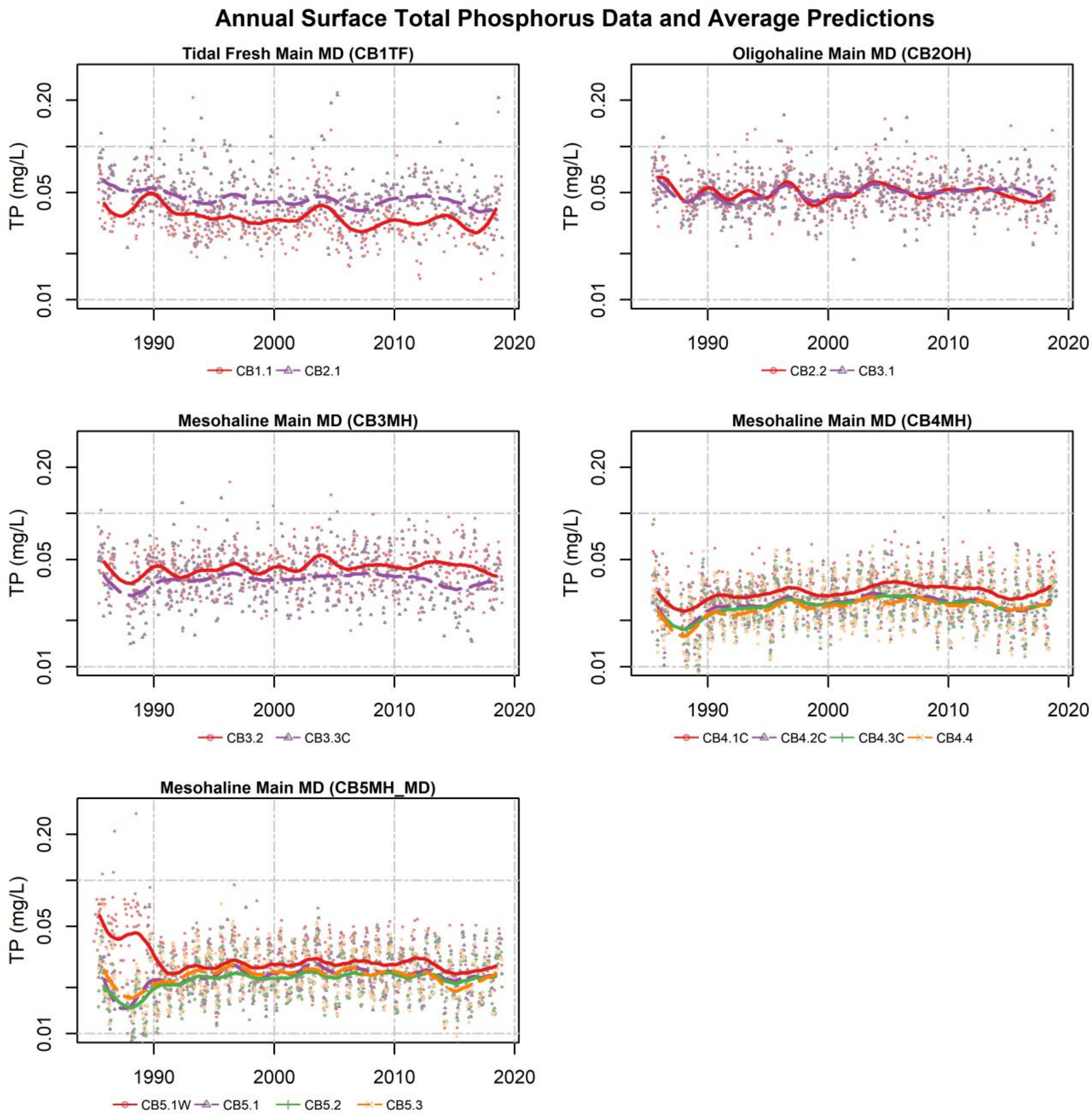

Figure 9. Surface TP data (dots) and average long-term pattern generated from non-flow adjusted GAMs. Colored dots represent data corresponding to the monitoring station indicated in the legend; colored lines represent mean annual GAM estimates for the noted monitoring stations.

The pattern at most of the mesohaline stations involves an initial drop followed by an increase until just before 2010 (Figure 9), resulting in the different long-term trend direction at the mesohaline stations compared to the tidal fresh stations in Figure 8. CB5.1W has a large decrease at the beginning of the record (Figure 9) which drives the improving trend found for that station (Figure 8) and is likely due to its proximity to the Patuxent River.

4.3 Surface Chlorophyll *a:* Spring (March-May)

Trends for chlorophyll *a* are split into spring and summer to analyze chlorophyll *a* during the two seasons when phytoplankton blooms are commonly observed in different parts of Chesapeake Bay (Smith and Kemp, 1995; Harding and Perry, 1997). Long-term spring chlorophyll *a* trends are degrading, both with and without flow-adjustment at the group of stations in the middle of this region. Over the short-term, most of those stations have no trend. The four most upper bay stations have improving or no trends with and without flow-adjustment over the long- and short-term. The lower two (CB5.2 and CB5.3) have no trend or mixed possible trends.

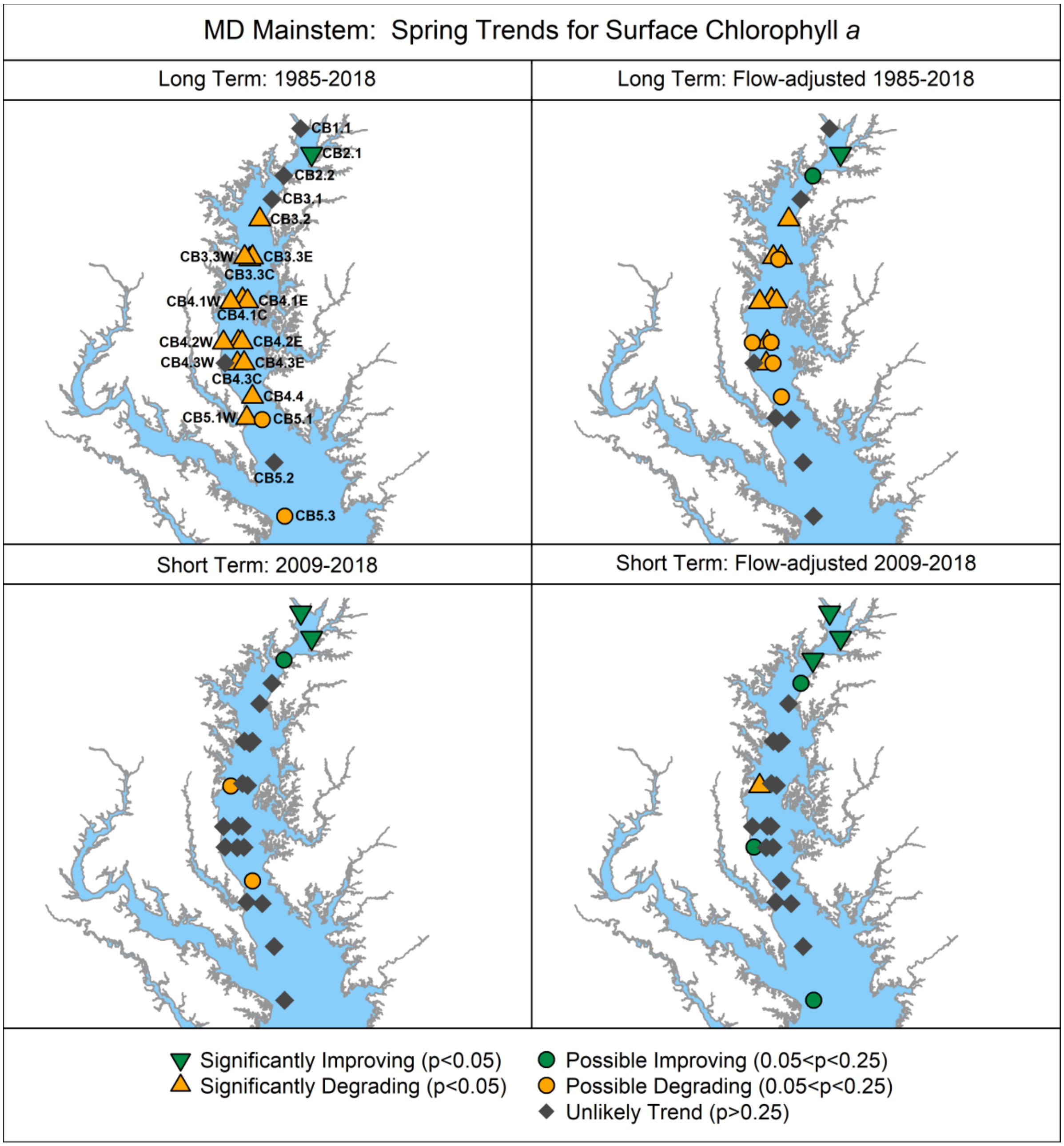

Figure 10. Surface spring (March-May) chlorophyll *a* trends. Base map credit Chesapeake Bay Program, www.chesapeakebay.net, North American Datum 1983.

Spring chlorophyll *a* concentrations dip down at the end of this record at all the tidal fresh and oligohaline stations (Figure 11). At the mesohaline stations, a gradual increase over the record is apparent in the data values and the mean spring GAM estimates.

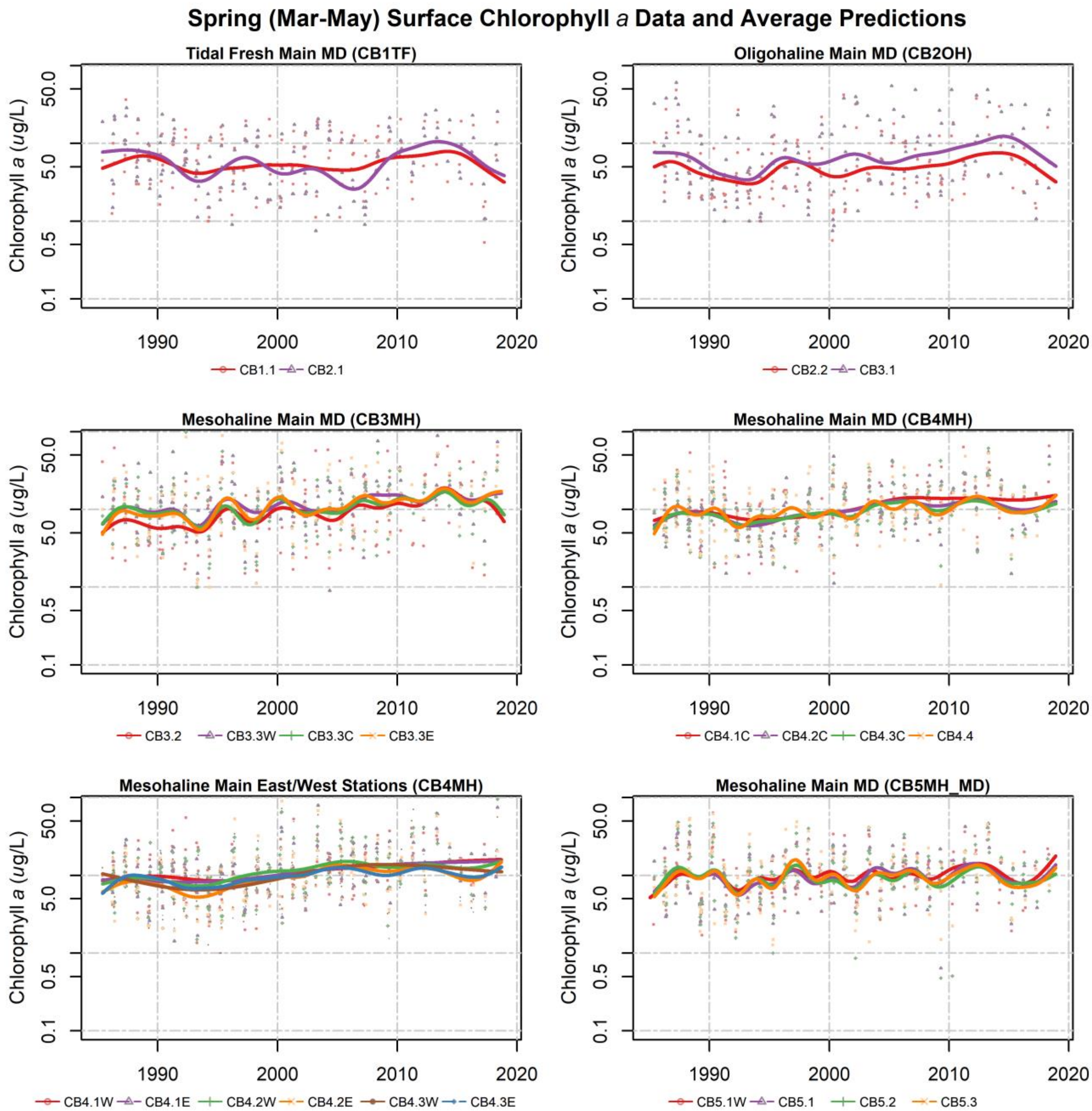

Figure 11. Surface spring chlorophyll *a* data (dots) and average long-term pattern generated from non-flow adjusted GAMs. Colored dots represent March-May data corresponding to the monitoring station indicated in the legend; colored lines represent mean spring GAM estimates for the noted monitoring stations.

4.4 Surface Chlorophyll *a:* Summer (July-September)

The spatial patterns in summer chlorophyll *a* trends (Figure 12) are similar to spring (Figure 10) except that there are more improving trends in the upper bay over the long-term in summer and more possible degradations over the short-term in summer at the middle group of stations (Figure 12).

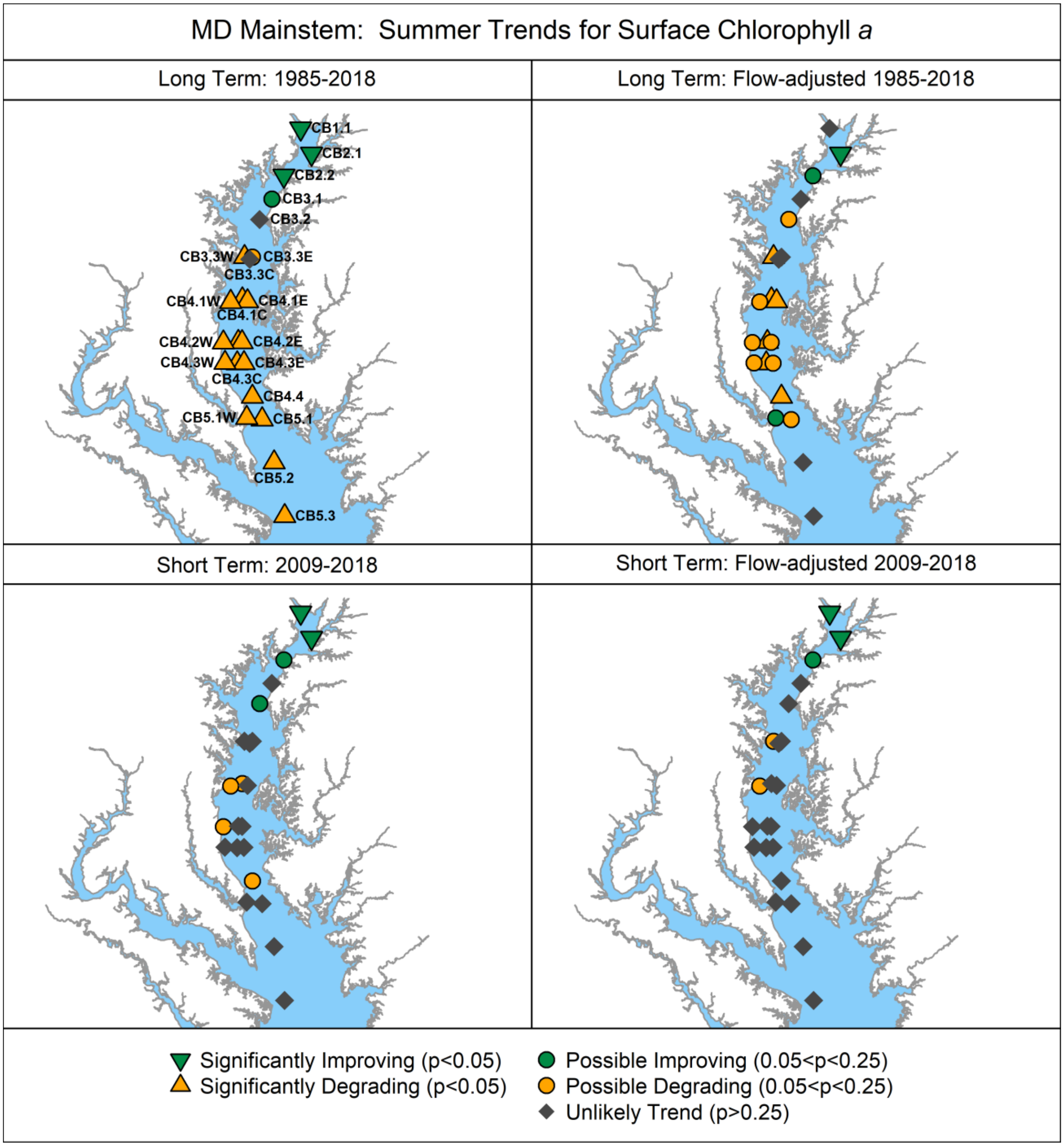

Figure 12. Surface summer (July-September) chlorophyll *a* trends. Base map credit Chesapeake Bay Program, www.chesapeakebay.net, North American Datum 1983.

The data values and mean summer GAM estimates dip down at the end of the record in the tidal fresh and oligohaline stations (Figure 13), similar to the observations made for the spring (Figure 11). Likewise, the mesohaline stations show increases over time (Figure 13).

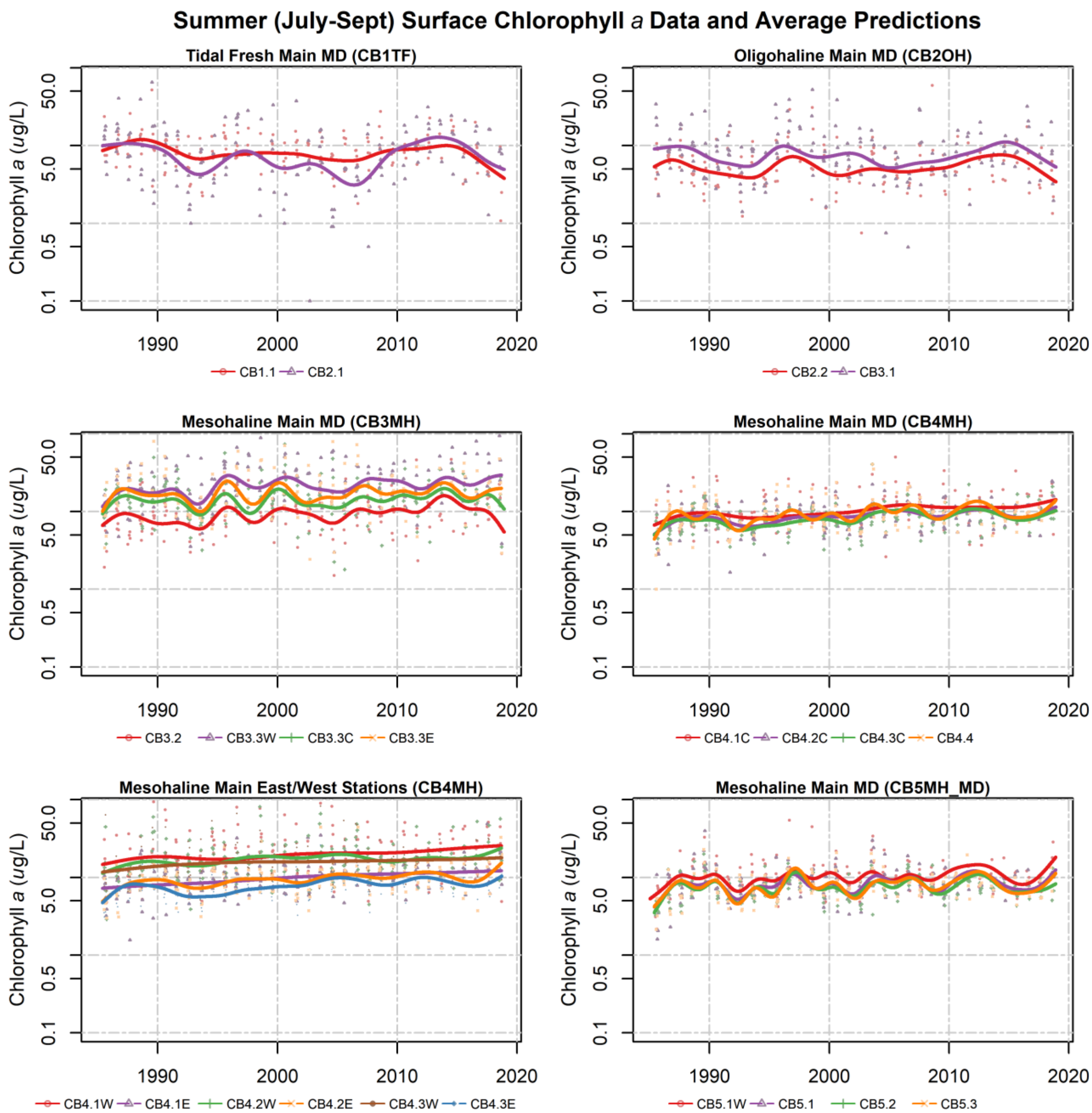

Figure 13. Surface summer chlorophyll *a* data (dots) and average long-term pattern generated from non-flow adjusted GAMs. Colored dots represent July-September data corresponding to the monitoring station indicated in the legend; colored lines represent mean summer GAM estimates for the noted monitoring stations.

4.5 Secchi Disk Depth

Trends in Secchi disk depth, a measure of visibility through the water column, are degrading over the long-term, both with and without flow-adjustment, at most stations shown here (Figure 14). There are two improving trends over the long-term after flow-adjustment in the upper bay. Over the short-term, there are mostly no trends without flow-adjustment and a majority of improving trends with flow-adjustment (Figure 14).

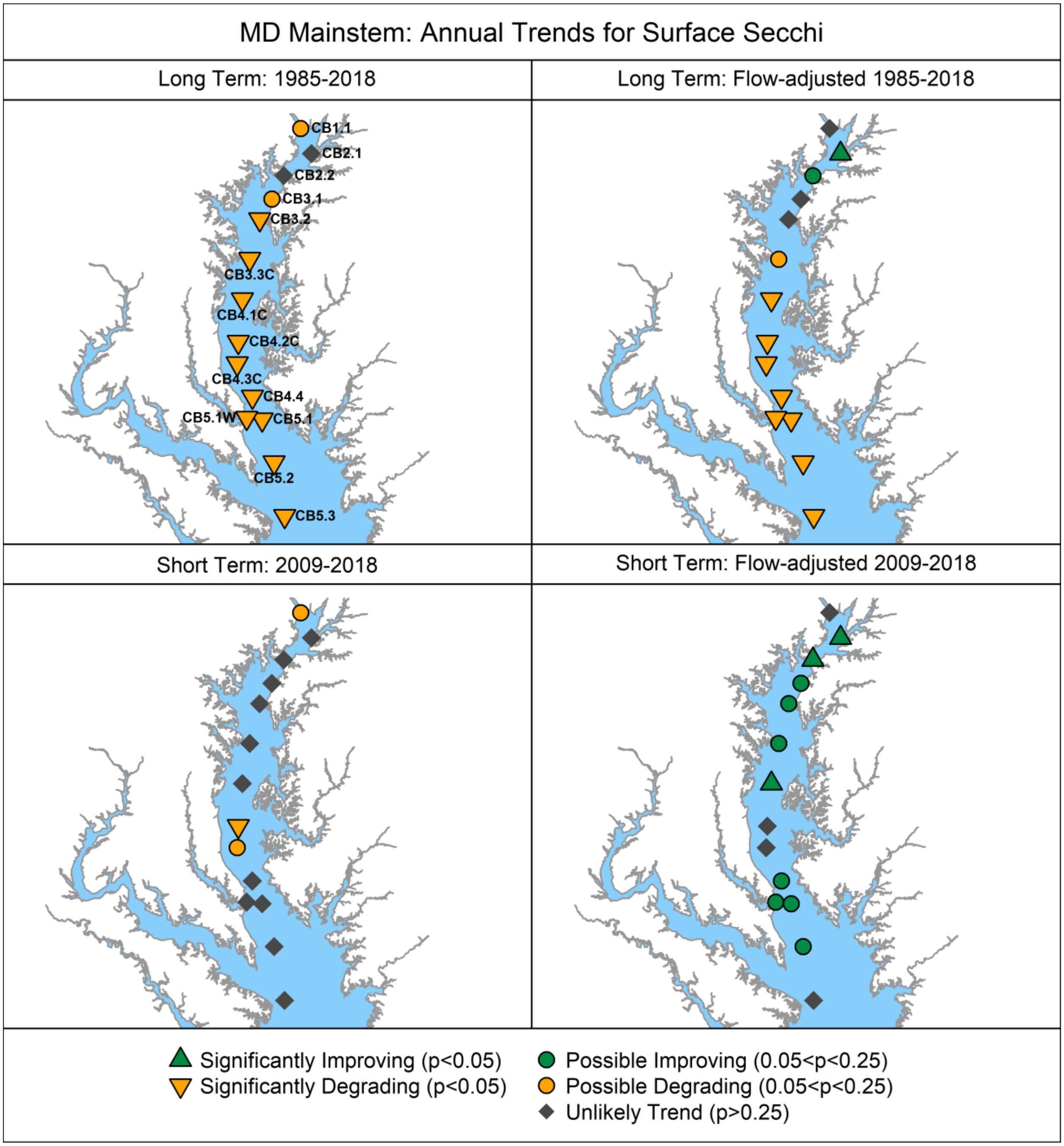

Figure 14. Annual Secchi depth trends. Base map credit Chesapeake Bay Program, www.chesapeakebay.net, North American Datum 1983.

Secchi depths are shallower throughout the entire record at the tidal fresh and oligohaline stations than the mesohaline stations (Figure 15). Long-term decreases are, however, much more apparent at the mesohaline stations. The decreases at most stations appear to level-out in the last half of the record.

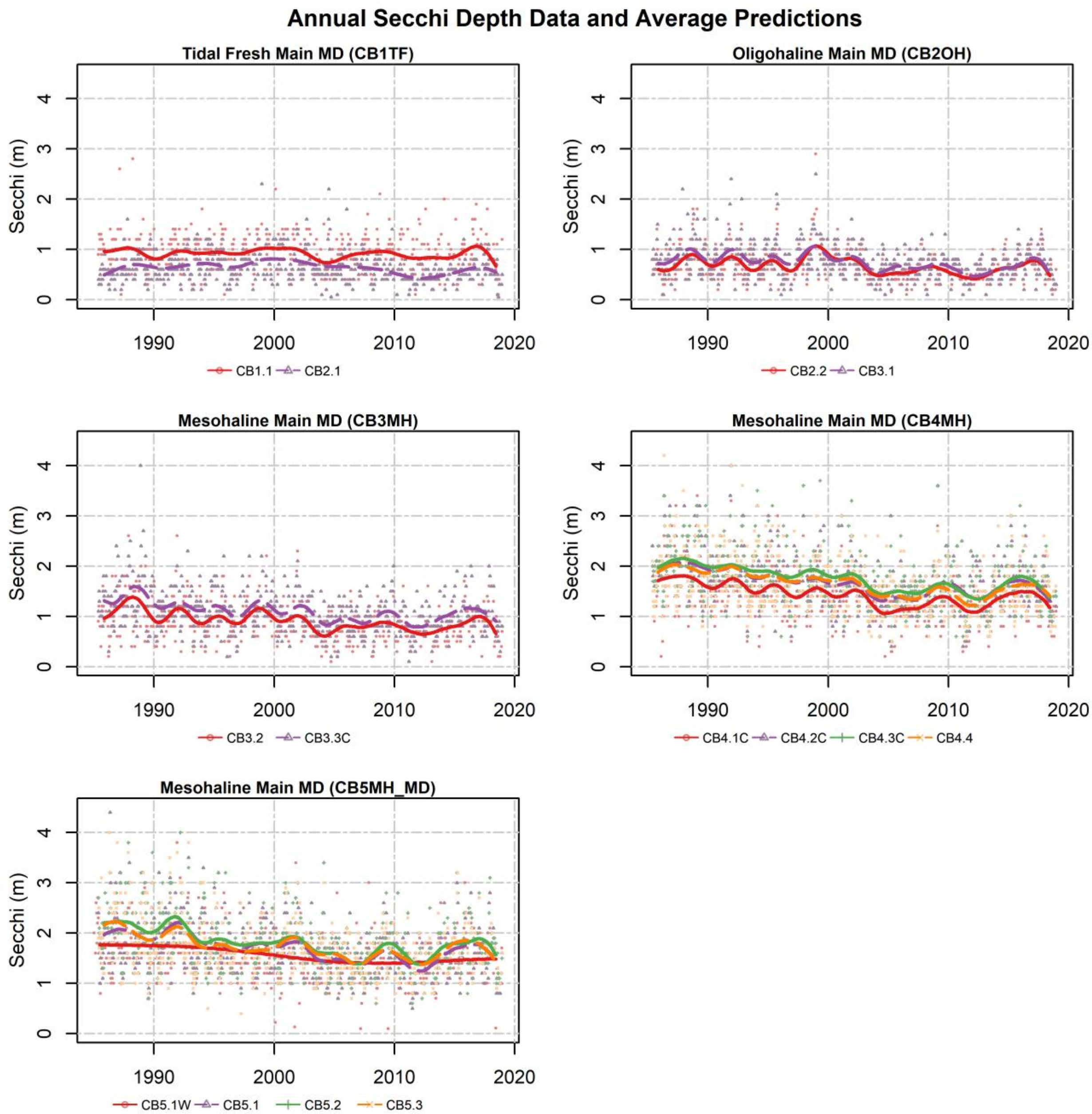

Figure 15. Annual Secchi depth data (dots) and average long-term pattern generated from non-flow adjusted GAMs. Colored dots represent data corresponding to the monitoring station indicated in the legend; colored lines represent mean annual GAM estimates for the noted monitoring stations.

4.6 Summer Bottom Dissolved Oxygen (June-September)

Summer bottom oxygen concentrations are improving at the majority of the stations over the long-term, both with and without flow-adjustment (Figure 16). All other stations show no long-term trend with the exception of a degrading trend at CB5.1W. Over the short-term, there are slightly fewer improving trends, but a clear spatial group of them in the lower half of the region.

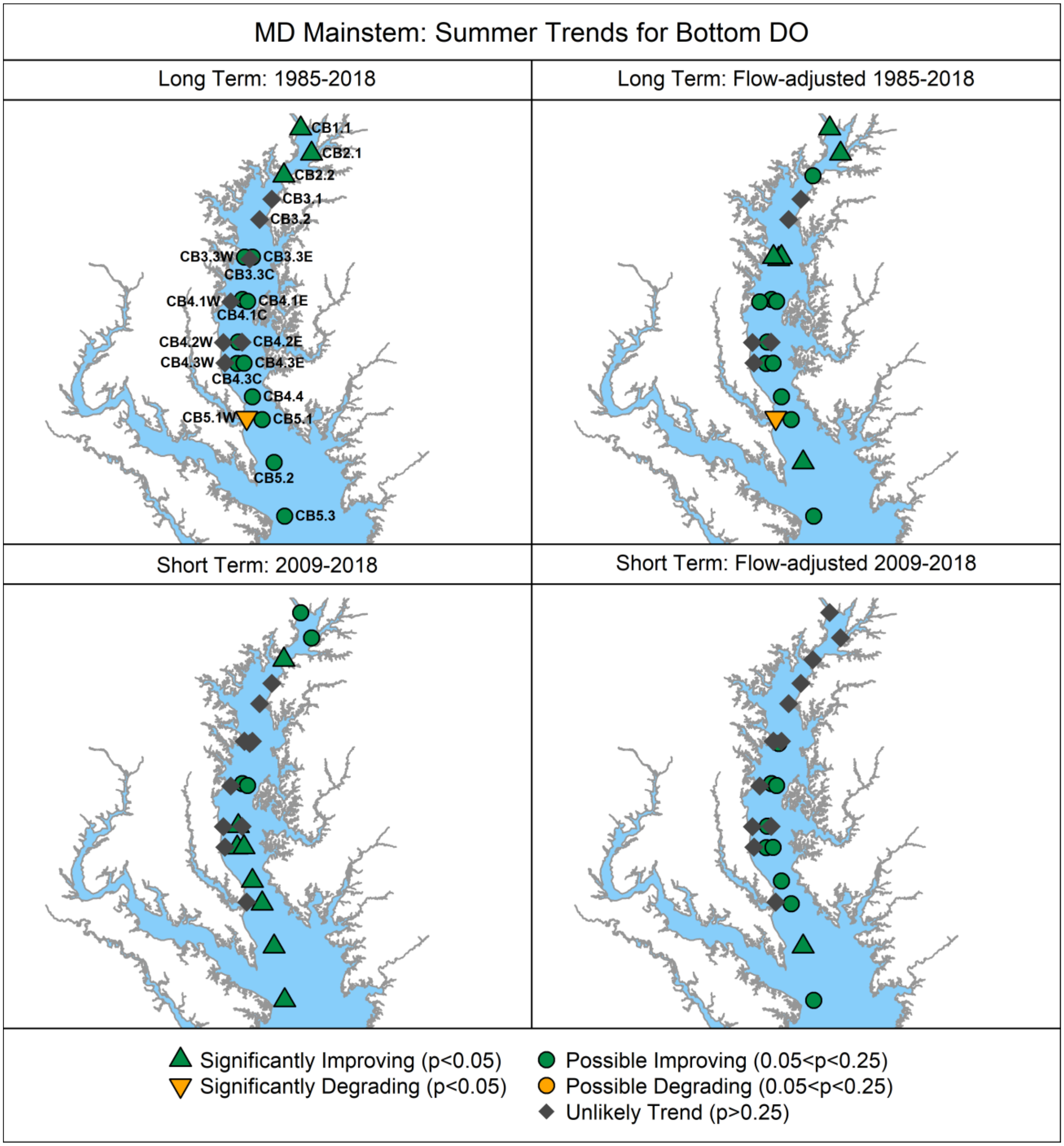

Figure 16. Summer (June-September) bottom DO trends. Base map credit Chesapeake Bay Program, www.chesapeakebay.net, North American Datum 1983.

Bottom oxygen concentrations are highest at the tidal fresh stations and lowest at the deep center channel stations in the mesohaline (Figure 17). Increases over time are apparent in many of these records both in the DO observations and the mean summer GAM estimates. Improvements in most of the lowest DO records appear to be an upswing in the last 10 years. The only degrading trend (Figure 16) at CB5.1W is driven in large part by a decrease at the beginning of the record (Figure 17).

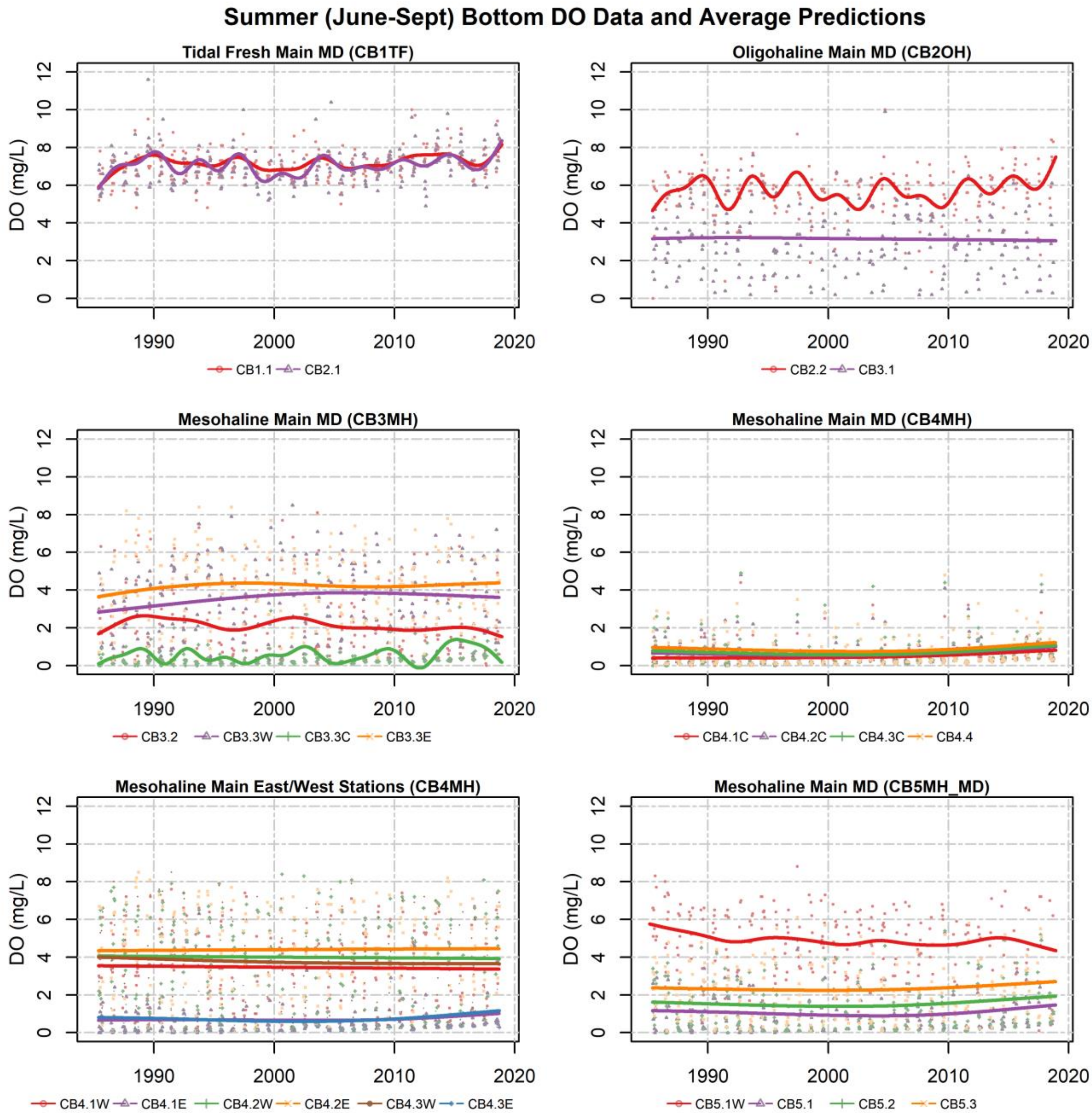

Figure 17. Summer (June-September) bottom DO data (dots) and mean summer long-term pattern generated from non-flow adjusted GAM. Colored dots represent June-September data corresponding to the monitoring station indicated in the legend; colored lines represent mean summer GAM estimates for the noted monitoring stations.

5. Factors Affecting Trends

5.1 Watershed Factors

5.1.1 Effects of Physical Setting

The geology of the Maryland Mainstem watershed and its associated land use affects the quantity and transfer of nitrogen, phosphorus, and sediment delivered to non-tidal and tidal streams (Figure 18) (Brakebill *et al.*, 2010; Ator *et al.*, 2011; Ator *et al.*, 2019; Ator *et al.*, 2020; Noe *et al.*, 2020).

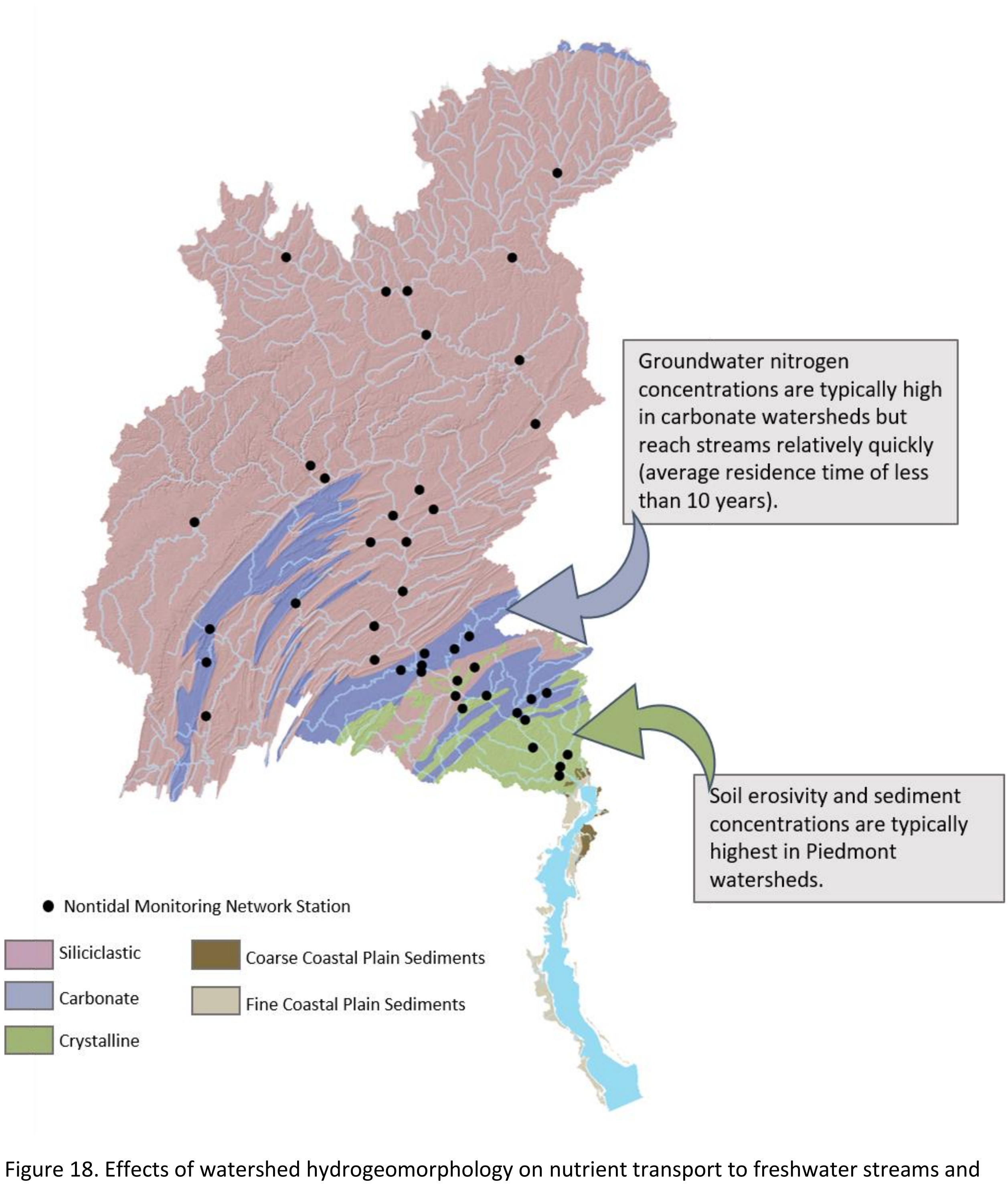

Figure 18. Effects of watershed hydrogeomorphology on nutrient transport to freshwater streams and tidal waters. Base map modified from King *et al.* (1974) and Ator *et al.* (2005), North American Datum 1983.

Nitrogen

Groundwater is an important delivery pathway of nitrogen, as nitrate, to most streams in the Chesapeake Bay watershed (Ator and Denver, 2012; Bachman and others). The proportion of nitrogen in groundwater that reaches freshwater streams and/or tidal waters is heavily dependent on location in the watershed. Concentrations of groundwater nitrogen, primarily as nitrate, are typically highest in the Maryland Mainstem watershed in portions of the ridge and valley and piedmont physiographic provinces that are underlain by carbonate geology (Greene and others, 2005; Terziotti and others, 2017). The geology of these areas provides suitable land for agriculture, but has little potential for denitrification (Böhlke and Denver, 1995; Sanford and Pope, 2013), so nitrogen that is not removed by plants or exported in agricultural products can move relatively efficiently to groundwater (where denitrification can occur as well) and to streams. The typical residence time of groundwater delivered to streams in the Chesapeake Bay watershed is about 10 years, but ages vary from less than 1 year to greater than 50 years based on bedrock structure, groundwater flow paths, and aquifer depths (Lindsey and others, 2003). In general, groundwater ages tend to be relatively short (0-10 years) in carbonate settings, where permeable soils and solution-enlarged fractures enhance groundwater connectivity (Lindsey and others, 2003). Groundwater represents about 50% of streamflow in most Chesapeake Bay streams, with the other half composed of soil moisture and runoff, which have residence times of days to months (Phillips, 2007).

Phosphorus

Phosphorus binds to soil particles and most phosphorus delivered to the Bay is attached to sediment (Zhang *et al.*, 2015); however, once fully phosphorus-saturated soils will not retain new applications and export of dissolved phosphorus to streams, from shallow soils and groundwater, will increase (Staver and Brinsfield, 2001). Phosphorus sorption capacity varies based on soil particle chemical composition and physical structure with clays typically having the greatest number of sorption sites and highest average phosphorus concentrations (Sharpley, 1980). The highest soil phosphorus concentrations in the Maryland Mainstem watershed typically occur in agricultural areas (Ator *et al.*, 2011) where inputs of manure and fertilizer exceed crop needs. Some sedimentary rocks in the upper Maryland Mainstem Watershed contain large phosphorus reservoirs (Terziotti, 2019), and while these natural sources contribute to in-stream loads, most is insoluble and only represent a dominant source in undeveloped watersheds. Reducing soil phosphorus concentrations can take multiple decades (Kleinman *et al.*, 2011) and, until this occurs, watershed phosphorus loads may appear to be unresponsive to management practices (Jarvie *et al.*, 2013; Sharpley *et al.*, 2013).

Sediment

The delivery of sediment from upland soil erosion, streambank erosion, and tributary loading varies throughout the Maryland Mainstem watershed, but in-stream concentrations are typically highest in Piedmont watersheds (Brakebill *et al.*, 2010). The erosivity of Piedmont soils results from its unique topography and from the prevalence of agricultural and urban land uses (Trimble, 1975; Gellis *et al.*, 2005; Brakebill *et al.*, 2010). Factors affecting streambank erosion are highly variable throughout the Maryland Mainstem watershed and include drainage area, bank sediment density, vegetation, stream valley geomorphology, and developed land uses (Wynn and Mostaghimi, 2006; Brakebill *et al.*, 2010; Gellis and Noe, 2013; Gellis *et al.*, 2015; Gillespie *et al.*, 2018; Hopkins *et al.*, 2018).

Delivery to tidal waters from the non-tidal watershed

The delivery of nitrogen, phosphorus, and sediment in non-tidal Maryland Mainstem streams to tidal waters varies based on physical and chemical factors that affect in-stream retention, loss, or storage. In general, nutrient and sediment loads in tidal waters are most strongly influenced by conditions in proximal non-tidal streams that have less opportunity for denitrification and floodplain trapping of sediment- associated phosphorus. In-stream denitrification rates vary spatially and temporally throughout the Maryland Mainstem watershed and typically increase with soil moisture and temperature (Pilegaard, 2013). There are no chemical processes to remove phosphorus or sediment from streams, but sediment, and associated phosphorus, can be stored behind impoundments or trapped in floodplains before reaching tidal waters. Sediment is stored behind three reservoirs in the lower Maryland Mainstem, but delivery of sediment to the Bay has increased since the late 1990s due to sediment infill of the Conowingo Reservoir (Hirsch, 2012; Zhang *et al.*, 2013; Langland, 2015; Zhang *et al.*, 2016).

5.1.2 Estimated Nutrient and Sediment Loads

Estimated loads to tidal portions of Chesapeake Bay tributaries are a combination of monitored fluxes from U.S. Geological Survey (USGS) River Input Monitoring (RIM) stations located at the nontidal-tidal interface and below-RIM simulated loads from the Chesapeake Bay Program Watershed Model. Nitrogen, phosphorus, and suspended sediment loads to the tidal Maryland Mainstem were primarily from the RIM areas (Figure 19). Over the period of 1985-2018, 2.3, 0.11, and 107 million tons of nitrogen, phosphorus, and suspended sediment loads were exported to the Maryland Mainstem, with 91%, 86%, and 60% of those loads from the RIM areas, respectively.

Mann-Kendall trends and Sen's slope estimates are summarized for each loading source in Table 4.

Nitrogen

Estimated TN loads showed an overall decline of -368 ton/yr in the period between 1985 and 2018, although it is statistically significant ($p = 0.31$). This reduction reflects a combination of reductions in RIM loads (-302 ton/yr; $p = 0.31$) and below-RIM loads (-47 ton/yr; $p < 0.01$). Within the below-RIM loads, significant reductions were observed with the point sources (-21 ton/yr, $p < 0.01$) and the atmospheric deposition to the tidal waters (-19 ton/yr, $p < 0.01$). The below-RIM nonpoint sources also showed a decline in this period (-17 ton/yr), although it is not statistically significant ($p = 0.17$). The significant below-RIM point source reductions in TN are a result of substantial efforts to reduce nitrogen loads from major wastewater treatment facilities by implementing biological nutrient removal (Boynton *et al.*, 2008; Lyerly *et al.*, 2014). The significant decline in atmospheric deposition of TN to the tidal waters is consistent with findings that atmospheric deposition of nitrogen has decreased due to benefits from the Clean Air Act implementation (Eshleman *et al.*, 2013; Lyerly *et al.*, 2014).

Phosphorus

Estimated TP loads showed an overall increase of 13 ton/yr in the period between 1985 and 2018, although it is not statistically significant ($p = 0.50$). This increase is largely driven by the RIM loads (15 ton/yr, $p = 0.44$). Within the below-RIM load, point sources showed a statistically significant decline in this period (-2.4 ton/yr; $p < 0.01$), whereas nonpoint sources showed a long-term increase (0.96 ton/yr, $p = 0.36$). This TP point source load reduction has also been attributed to significant efforts to reduce phosphorus in wastewater discharge through the phosphorus detergent ban in the early part of this record, as well as technology upgrades at wastewater treatment facilities (Boynton *et al.*, 2008; Lyerly *et al.*, 2014).

Sediment

Estimated suspended sediment (SS) loads showed an overall increase of 3,011 ton/yr in the period between 1985 and 2018, although it is not statistically significant ($p = 0.70$). Both the RIM and below-RIM loads showed long-term increases, but both are not statistically significant. Like TP and TN, the below-RIM point source load of SS showed a statistically significant decline in this period (-12 ton/yr; $p < 0.01$).

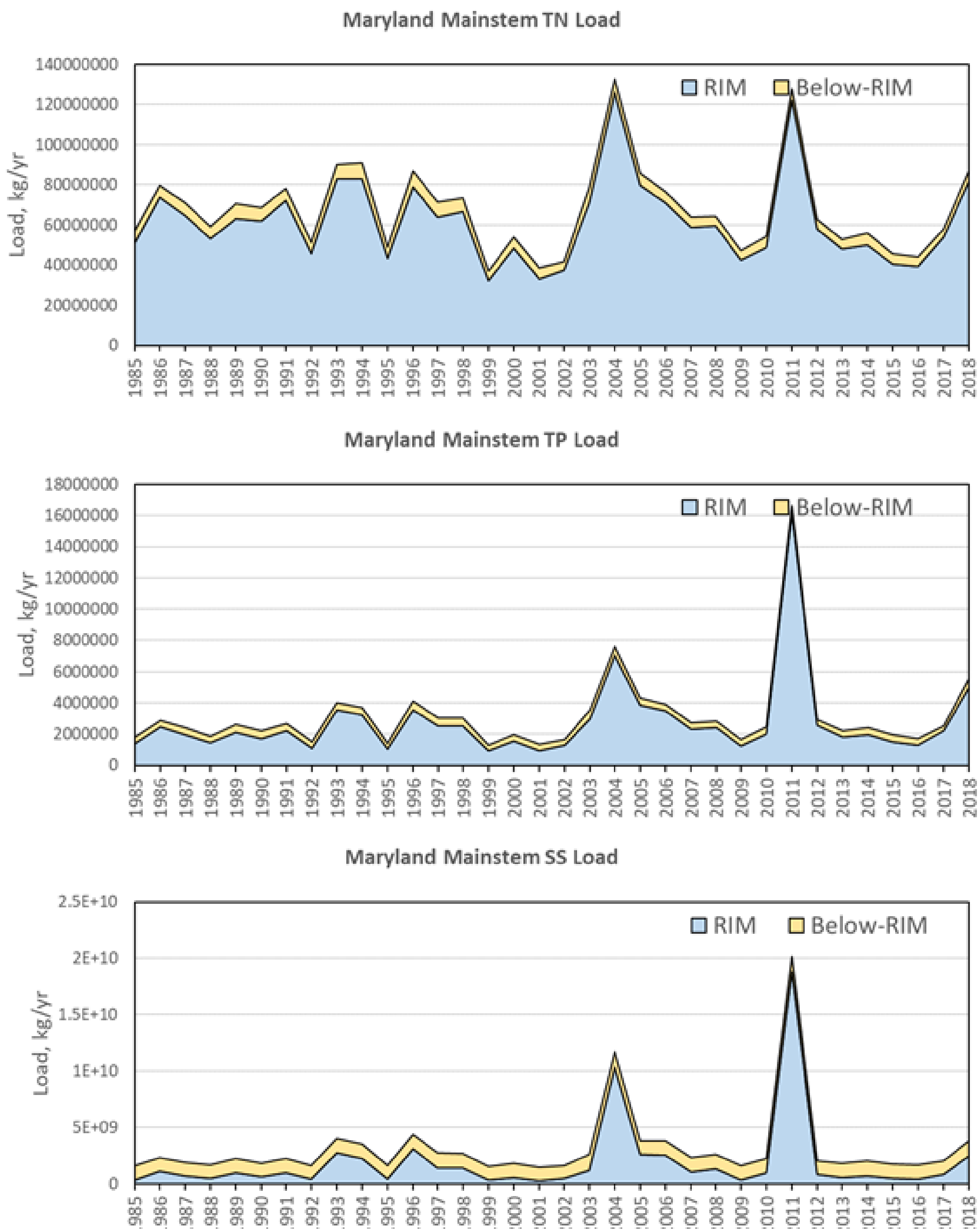

Figure 19. Estimated total loads of nitrogen (TN), phosphorus (TP), and suspended sediment (SS) from the RIM and below-RIM areas of the Maryland Mainstem. RIM refers to the USGS River Input Monitoring site (i.e., Susquehanna) located just above the head of tide of four tributaries. Below-RIM estimates are a combination of simulated non-point source, atmospheric deposition, and reported point-source loads.

Table 4. Summary of Mann-Kendall trends for the period of 1985-2018 for total nitrogen (TN), total phosphorus (TP), and suspended sediment (SS) loads to the Maryland Mainstem.

Variable	Trend, metric ton/yr	Trend p-value
TN		
Total watershed	-368	0.31
RIM watershed [1]	-302	0.31
Below-RIM watershed [2]	-47	< 0.01
Below-RIM point source	-21	< 0.01
Below-RIM nonpoint source [3]	-17	0.17
Below-RIM tidal deposition	-19	< 0.01
TP		
Total watershed	13	0.50
RIM watershed	15	0.44
Below-RIM watershed	-1.5	0.16
Below-RIM point source	-2.4	< 0.01
Below-RIM nonpoint source	0.96	0.36
SS		
Total watershed	3,011	0.70
RIM watershed	3,489	0.74
Below-RIM watershed	1,596	0.08
Below-RIM point source	-12	< 0.01
Below-RIM nonpoint source	1,616	0.08

[1] Loads for the RIM watershed were estimated loads at the USGS RIM station 01578310 (Susquehanna River at Conowingo, Md.) (https://cbrim.er.usgs.gov/loads_query.html).
[2] Loads for the below-RIM watershed were obtained from the Chesapeake Bay Program Watershed Model (https://cast.chesapeakebay.net/).
[3] Below-RIM nonpoint source loads were obtained from the Chesapeake Bay Program Watershed Model's progress runs specific to each year from 1985 and 2018, which were adjusted to reflect actual hydrology using the method of the Chesapeake Bay Program's Loads to the Bay indicator (see https://www.chesapeakeprogress.com/clean-water/water-quality).

5.1.3 Expected Effects of Changing Watershed Conditions

According to the Chesapeake Bay Program's Watershed Model known as the Chesapeake Assessment Scenario Tool (CAST; https://cast.chesapeakebay.net, version CAST-2019), changes in population size, land use, and pollution management controls between 1985 and 2019 would be expected to change long-term average nitrogen, phosphorus, and sediment loads to the tidal Maryland Mainstem River by -13%, -37%, and -12%, respectively (Figure 20). In contrast to the annual loads analysis above, CAST loads are based on changes in management only and do not include annual fluctuations in weather. CAST loads are calculated without lag times for delivery of pollutants or lags related to BMPs becoming fully effective after installation. In 1985, agriculture and wastewater were the two largest sources of nitrogen loads. By 2019, agriculture remained the largest nitrogen source; however, wastewater nitrogen loads had changed by -30% and the developed sector had taken its place as the second largest nitrogen source. Overall, decreasing nitrogen loads from agriculture (-20%), stream bed and bank (-12%), and wastewater (-30%) sources were partially counteracted by increases from developed (36%) and septic (22%) sources.

The two largest sources of phosphorus loads as of 2019 were the agriculture and wastewater sectors. Overall, expected declines from agriculture (-39%), stream bed and bank (-34%), and wastewater (-63%) sources were partially counteracted by increases from developed (31%) sources.

For sediment, the largest sources are shoreline and stream bed and bank areas: these two sources changed by 0% and -16%, respectively between 1985 and 2019. Sediment loads from the agriculture sector changed by -40%, whereas sediment load from developed areas changed by 15%.

Overall, changing watershed conditions are expected to result in the agriculture, stream bed and bank, and wastewater sectors achieving reductions in nitrogen, phosphorus, and sediment loads between 1985 and 2019, whereas the developed sectors are expected to increase in nitrogen, phosphorus, and sediment loads.

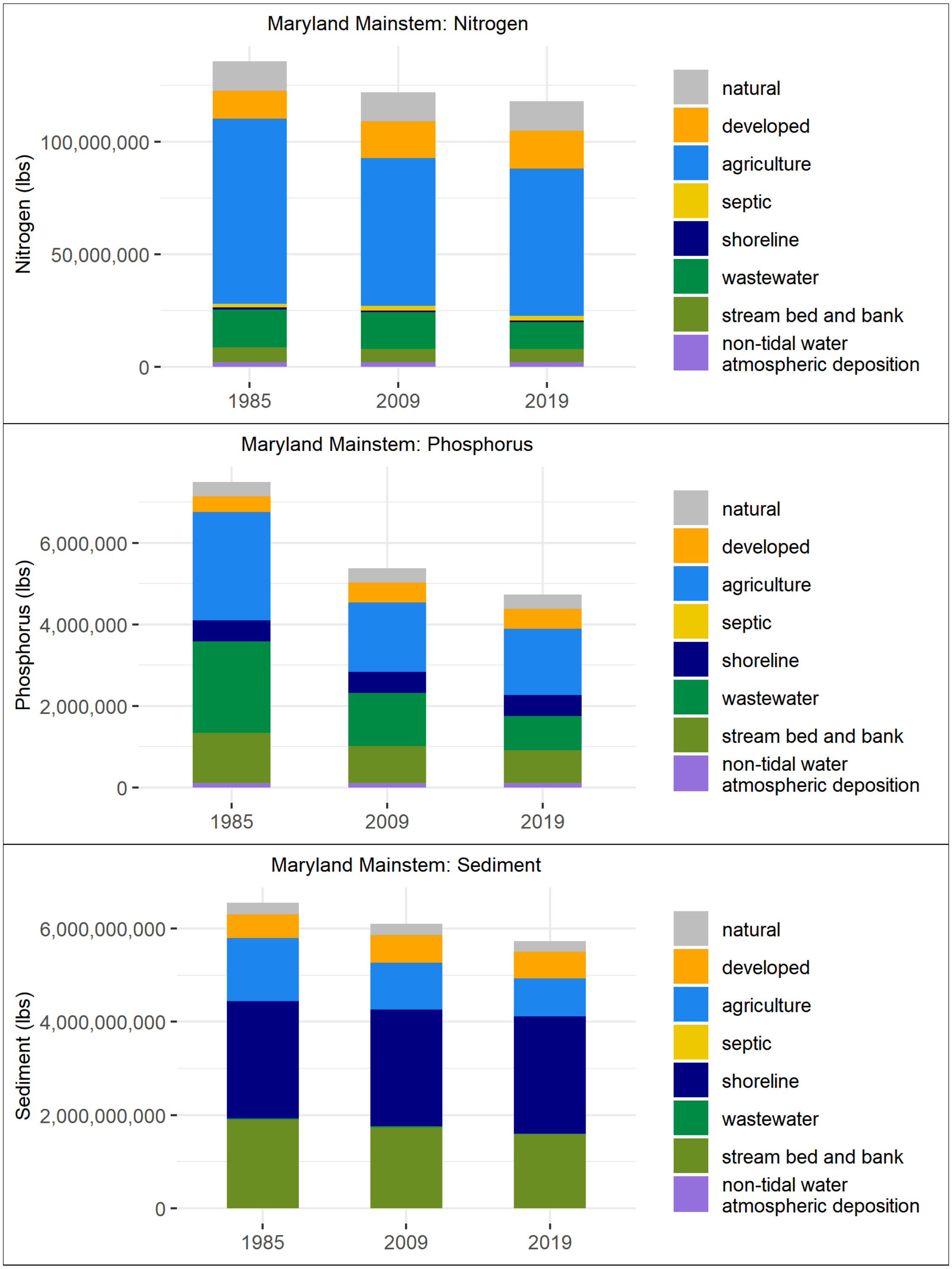

Figure 20. Expected long-term average loads of nitrogen, phosphorus, and sediment from different sources to the Maryland Mainstem, as obtained from the Chesapeake Assessment Scenario Tool (CAST-19). Data shown are time-average delivered loads over the average hydrology of 1991-2000, once the steady state is reached for the conditions on the ground, as obtained from the 1985, 2009, and 2018 progress (management) scenarios.

5.1.4 Best Management Practices (BMPs) Implementation

Data on reported BMP implementation are available for download from CAST (https://cast.chesapeakebay.net, version CAST-2019). Reported BMP implementations on the ground as of 1985, 2009, and 2019 are compared to planned 2025 implementation levels in Figure 21 for a subset of major BMP groups measured in acres. As of 2019, tillage, cover crops, pasture management, forest buffer and tree planting, stormwater management, agricultural nutrient management, and urban nutrient management were credited for 1,201, 245, 111, 0.7, 88, 1,125, and 48 thousand acres, respectively. Implementation levels for some practices are already close to achieving their planned 2025 levels: for example, 106% of planned acres for tillage had been achieved as of 2019. In contrast, about 34% of planned commodity & cover crops implementation had been achieved as of 2019.

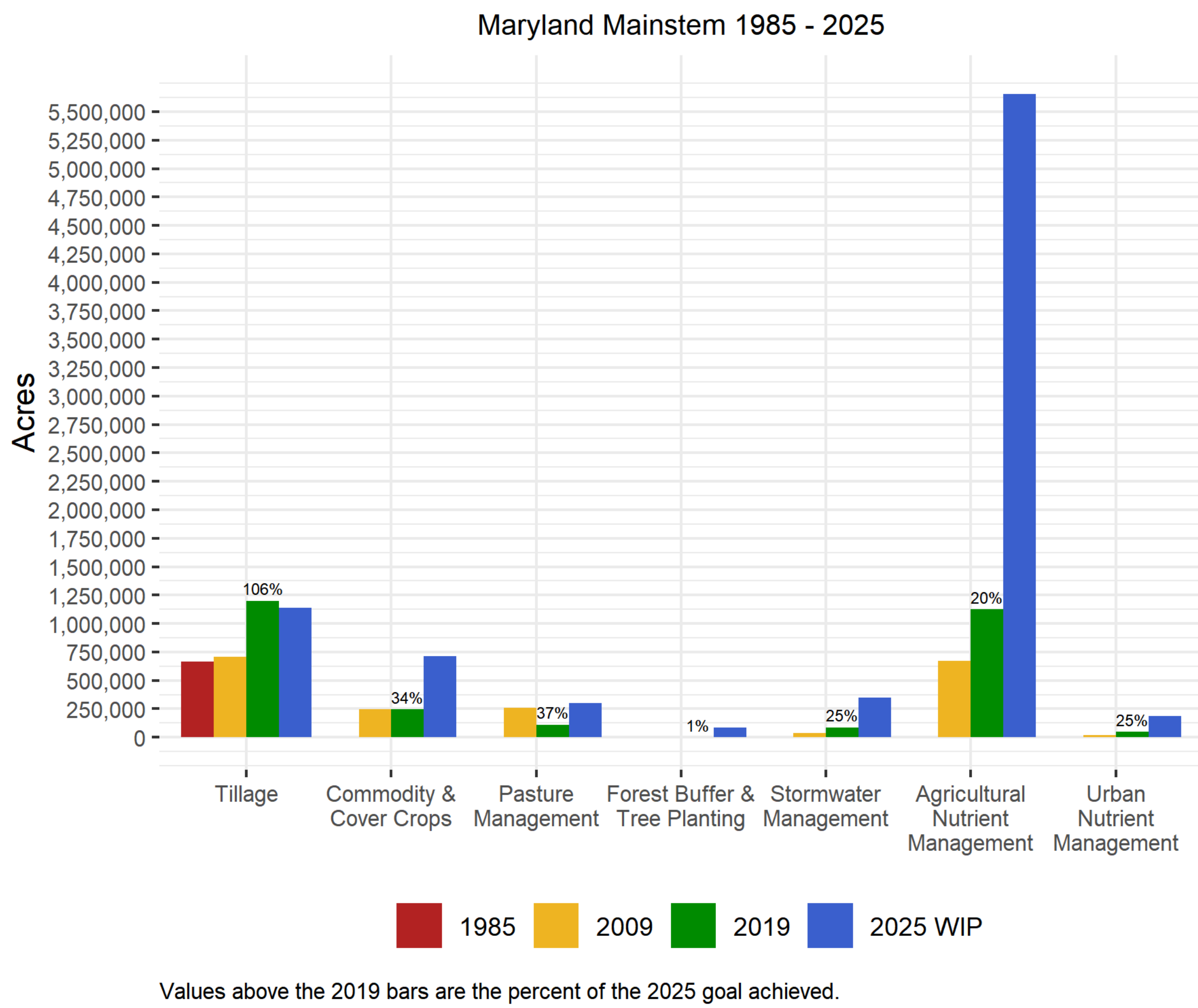

Figure 21. BMP implementation in the Maryland Mainstem watershed

Stream restoration and animal waste management system systems are two important BMPs that cannot be compared directly with those above because they are measured in different units. However, progress towards implementation goals can still be documented. Stream restoration (agricultural and urban) had increased from 0 feet in 1985 to 518,797 feet in 2019. Over the same period, animal waste management systems treated 1,320 animal units in 1985 and 1,131,118 animal units in 2019 (one animal unit represents 1,000 pounds of live animal). These implementation levels represent 33% and 51% of their planned 2025 implementation levels, respectively.

5.1.5 Flow-Normalized Watershed Nutrient and Sediment Loads

Flow normalization can better reveal temporal trends in river water quality by removing the effect of inter-annual variability in streamflow. Flow-normalized trends help scientists evaluate changes in load resulting from changing sources, delays associated with storage or transport of historical inputs, and/or implemented management actions. Flow-normalized nitrogen, phosphorus, and sediment trends have been reported for the long term (1985-2019) and short term (2009-2018) at nontidal network stations throughout the watershed (Moyer and Langland, 2020) (Table 5). These trends result from variability in nutrient applications, the delivery of nutrients and sediment from the landscape to streams, and from processes that affect in-stream loss or retention of nutrients and sediment.

Table 5. Long-term (1985 - 2018) and short-term trends (2009 - 2018) of flow-normalized total nitrogen (TN), total phosphorus (TP), and suspended sediment (SS) loads for nontidal network monitoring locations in the Maryland Mainstem watershed. A more detailed summary of flow-normalized loads and trends measured at all USGS Chesapeake Bay Nontidal Network stations can be found at https://cbrim.er.usgs.gov/summary.html.

USGS Station ID	USGS Station Name	Trend start water year	Percent change in FN load, through water year 2018		
			TN	TP	SS
01502500	UNADILLA RIVER AT ROCKDALE, NY	2009	0.9	**-26.2**	8.2
01503000	SUSQUEHANNA RIVER AT CONKLIN, NY	2009	**-11.1**	-5.2	**52.6**
01515000	SUSQUEHANNA RIVER NEAR WAVERLY, NY	2009	**4.2**	**0.0**	**71.5**
01529500	COHOCTON RIVER NEAR CAMPBELL, NY	2009	**7.7**	**-26.4**	**-12.4**
01531000	CHEMUNG RIVER AT CHEMUNG, NY	2009	**9.9**	**-32.4**	13.7
01531500	SUSQUEHANNA RIVER AT TOWANDA, PA	1989	**-39.8**	**23.8**	**11.9**
		2009	**9.3**	**48.0**	**75.6**
01534000	TUNKHANNOCK CREEK NEAR TUNKHANNOCK, PA	2009	**30.3**	**83.8**	**273.0**
01536500	SUSQUEHANNA RIVER AT WILKES-BARRE, PA	1989	**-41.6**		
		2009	3.5	11.6	**41.2**
01540500	SUSQUEHANNA RIVER AT DANVILLE, PA	1985	**-36.3**	**-9.8**	-3.4
		2009	**4.6**	**13.8**	**64.8**
01542500	WB SUSQUEHANNA RIVER AT KARTHAUS, PA	2009	**10.0**	**-8.2**	3.4
01549700	PINE CREEK BL L PINE CREEK NEAR WATERVILLE, PA	2009	**21.0**	**61.7**	**57.5**

01549760	WB SUSQUEHANNA RIVER NEAR JERSEY SHORE, PA	2009	8.6	7.7	27.5
01553500	WEST BRANCH SUSQUEHANNA RIVER AT LEWISBURG, PA	1985	-34.1	-35.6	-4.9
		2009	-5.5	-0.5	31.3
01555000	PENNS CREEK AT PENNS CREEK, PA	2009	13.6	-3.7	1.2
01562000	RAYSTOWN BRANCH JUNIATA RIVER AT SAXTON, PA	2009	10.9	32.0	43.9
01567000	JUNIATA RIVER AT NEWPORT, PA	1985	-19.8	-42.6	-45.5
		2009	2.3	-6.4	3.9
01568000	SHERMAN CREEK AT SHERMANS DALE, PA	2009	8.0	6.9	2.5
01570000	CONODOGUINET CREEK NEAR HOGESTOWN, PA	2009	-4.6	-7.0	-7.0
01571500	YELLOW BREECHES CREEK NEAR CAMP HILL, PA	2009	-9.2	34.6	114.0
01573560	SWATARA CREEK NEAR HERSHEY, PA	2009	-12.4	1.0	19.7
01574000	WEST CONEWAGO CREEK NEAR MANCHESTER, PA	2009	-7.2	12.1	3.8
01576000	SUSQUEHANNA RIVER AT MARIETTA, PA	1987	-32.2	-13.7	-20.3
		2009	-2.9	14.7	19.8
01576754	CONESTOGA RIVER AT CONESTOGA, PA	1985	-38.3	-49.6	-69.4
		2009	-18.1	15.6	17.6
01576787	PEQUEA CREEK NEAR MARTIC FORGE, PA	2009	-16.5	32.0	7.4
01578310	Susquehanna River at Conowingo, MD	1985	-21.8	24.4	53.1
		2009	-0.9	2.5	-28.3
01578475	OCTORARO CREEK NEAR RICHARDSMERE, MD	2009	-11.6	0.8	22.6
01580520	DEER CREEK NEAR DARLINGTON, MD	2009	-6.3	-5.2	30.6

Decreasing trends listed in green, increasing trends listed in orange, results reported as "no trend" listed in black. TN = total nitrogen, TP = total phosphorus, SS = suspended sediment

5.2 Tidal Factors

Once pollutants reach tidal waters, a complex set of environmental factors interact with them to affect key habitat indicators like algal biomass, DO concentrations, water clarity, submerged aquatic vegetation (SAV) abundance, and fish populations (Kemp *et al.*, 2005; Testa *et al.*, 2017) (Figure 22). For example, phytoplankton growth depends not just on nitrogen and phosphorus (Fisher *et al.*, 1992; Kemp *et al.*, 2005; Zhang *et al.*, 2021), but also on light and water temperature (Buchanan *et al.*, 2005; Buchanan, 2020). In general, the saline waters of the lower Bay tend to be more transparent than tidal-fresh regions, and waters adjacent to nutrient input points are more affected by these inputs than more distant regions (Keisman *et al.*, 2019; Testa *et al.*, 2019). Dissolved oxygen concentrations are affected by salinity- and temperature-driven stratification of the water column, and conversely by wind-driven mixing, in addition to phytoplankton respiration and decomposition (Scully, 2010; Murphy *et al.*, 2011). When anoxia occurs at the water-sediment interface, nitrogen and phosphorus stored in the sediments can be released through anaerobic chemical reactions (Testa and Kemp, 2012). When low-oxygen water and sediment burial suffocate benthic plant and animal communities, their nutrient consumption and water filtration services are lost. Conversely, when conditions improve enough to support abundant SAV and benthic communities, their functions can sustain and even advance progress towards a healthier ecosystem (Cloern, 1982; Phelps, 1994; Ruhl and Rybicki, 2010; Gurbisz and Kemp, 2014).

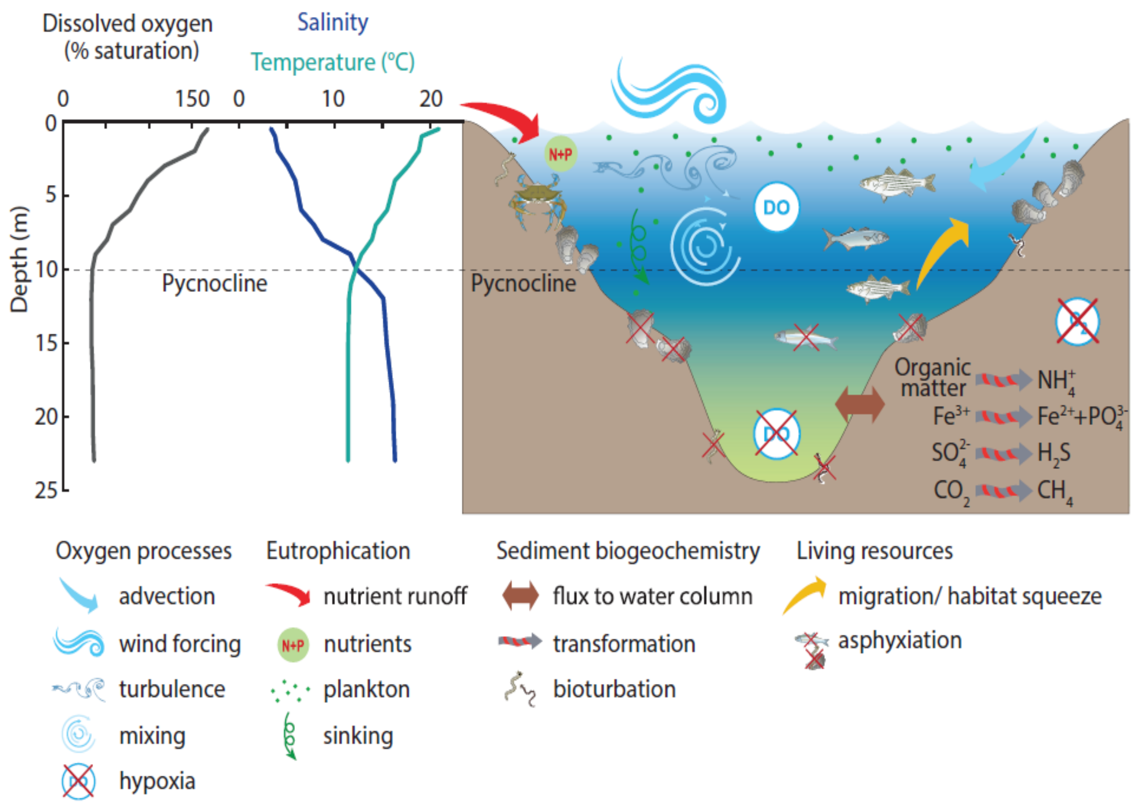

Figure 22. Conceptual diagram illustrating how hypoxia is driven by eutrophication and physical forcing, while affecting sediment biogeochemistry and living resources. From Testa *et al.* (2017).

High nutrient loads relative to tidal river size are indicative of areas that are more susceptible to eutrophication (Bricker *et al.*, 2003; Ferreira *et al.*, 2007). The relationship between watershed area and tidal river size may also be an important indicator of eutrophication potential, however there are competing effects. A large watershed relative to the volume of receiving water would likely correlate with higher nutrient loads, however it would also correlate with a higher flow rate and decreased flushing time (Bricker *et al.*, 2008). Figure 23 is a comparison of watershed area versus estuarine volume for all estuaries and sub-estuaries identified in the CBP monitoring segment scheme. Larger estuaries will contain multiple monitoring segments and, in many cases, sub-estuaries. For example, the Potomac River contains monitoring segments in the tidal fresh, oligohaline, and mesohaline sections of the river as well as the entire Anacostia River and other sub-estuaries. Figures 24 and 25 are comparisons of estimated annual average nitrogen and phosphorus loads, respectively, for the 2018 progress scenario in CAST versus the estuarine volume for the same set of estuaries and sub-estuaries.

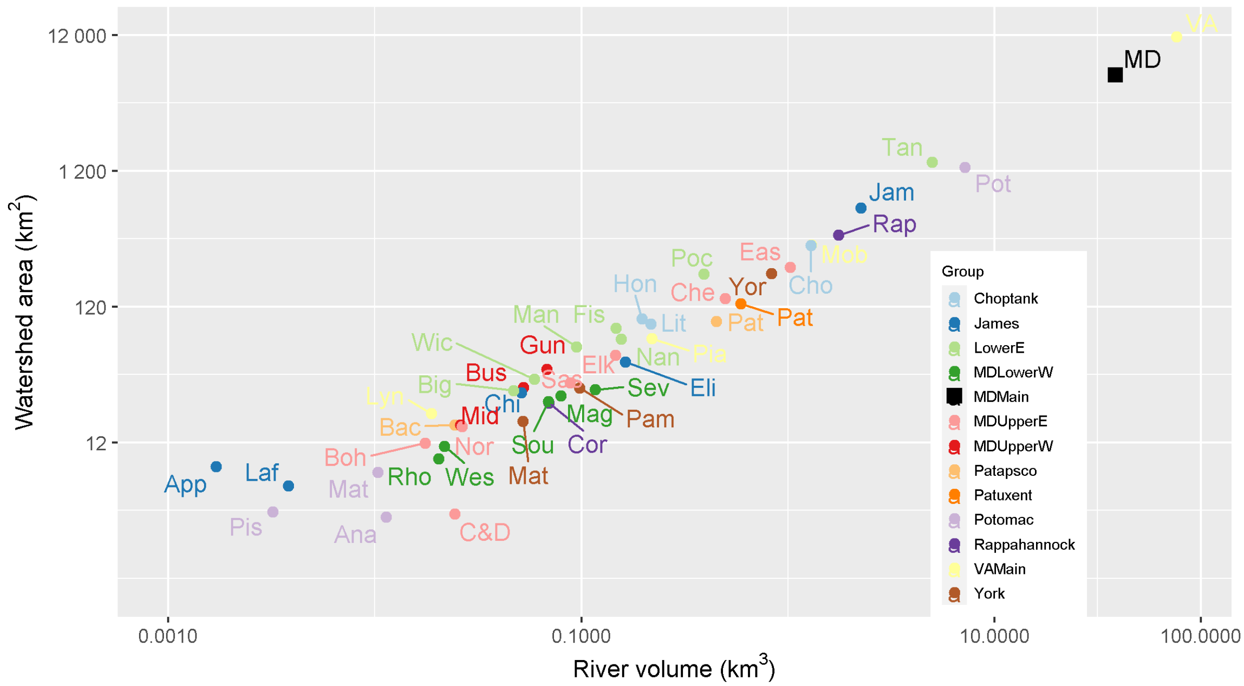

Figure 23. Watershed area vs estuarine volume.

Abbreviated tributary name	**Full tributary name**	**Abbreviated tributary name**	**Full tributary name**
Ana	Anacostia River	Mat	Mattaponi River
App	Appomattox River	MD	MD MAINSTEM
Bac	Back River	Mid	Middle River
Big	Big Annemessex River	Mob	Mobjack Bay
Boh	Bohemia River	Nan	Nanticoke River
Bus	Bush River	Nor	Northeast River
C&D	C&D Canal	Pam	Pamunkey River
Che	Chester River	Pat	Patapsco River
Chi	Chickahominy River	Pat	Patuxent River
Cho	Choptank River	Pia	Piankatank River
Cor	Corrotoman River	Pis	Piscataway Creek
Eas	Eastern Bay	Poc	Pocomoke River
Eli	Elizabeth River	Pot	Potomac River
Elk	Elk River	Rap	Rappahannock River
Fis	Fishing Bay	Rho	Rhode River
Gun	Gunpowder River	Sas	Sassafras River
Hon	Honga River	Sev	Severn River
Jam	James River	Sou	South River
Laf	Lafayette River	Tan	Tangier Sound
Lit	Little Choptank River	VA	VA MAINSTEM
Lyn	Lynnhaven River	Wes	West River
Mag	Magothy River	Wes	Western Branch (Patuxent River)
Man	Manokin River	Wic	Wicomico River
Mat	Mattawoman Creek	Yor	York River

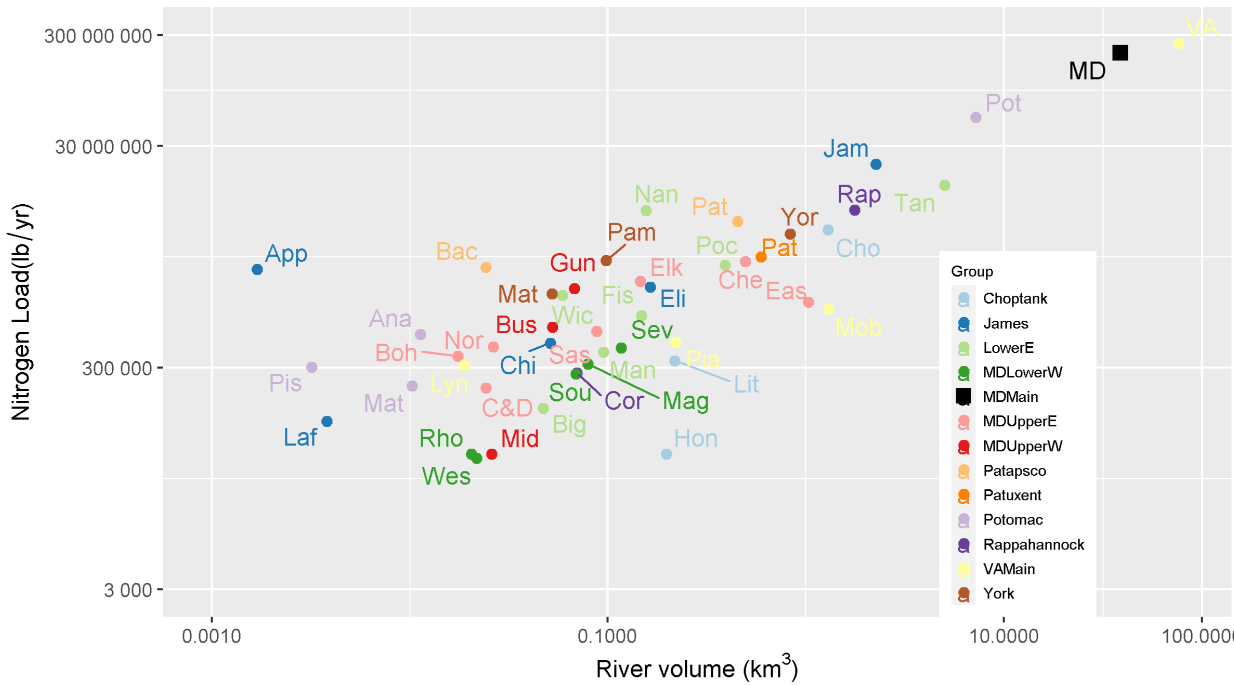

Figure 24. Annual average expected nitrogen loads versus estuarine volume. Nitrogen loads are from the 2018 progress scenarios in CAST (Chesapeake Bay Program, 2020), which is an estimate of nitrogen loads under long-term average hydrology given land use and reported management as of 2018.

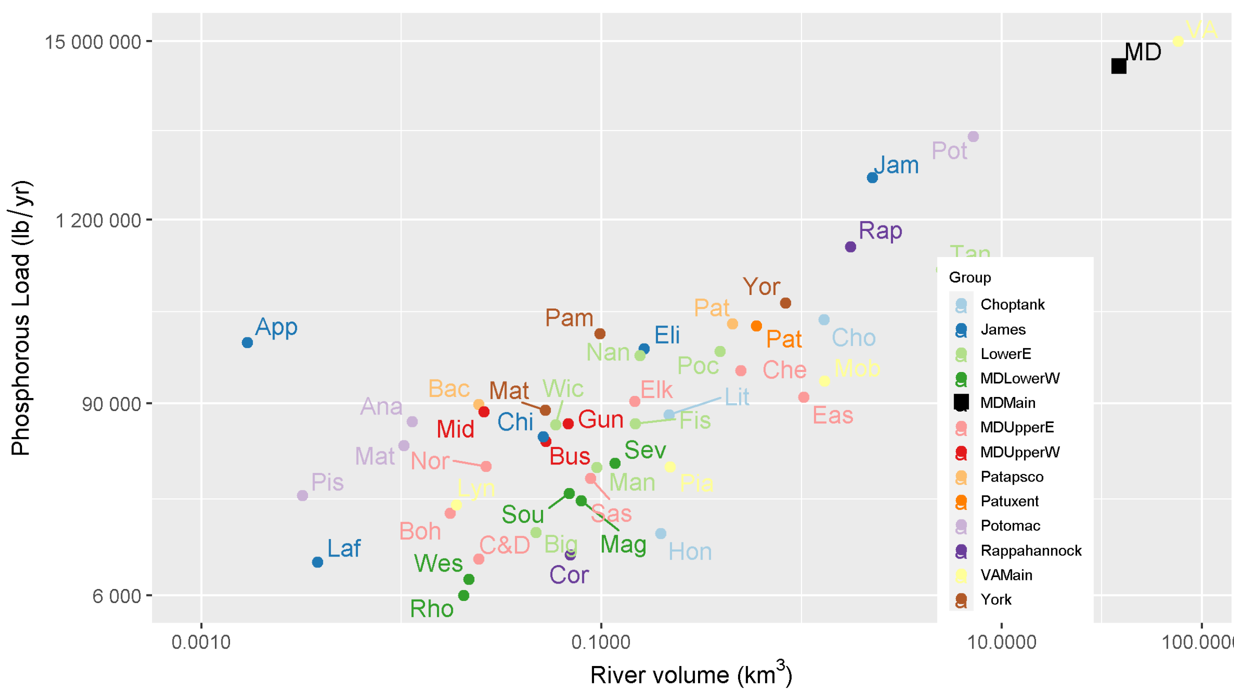

Figure 25. Annual average expected phosphorus loads versus estuarine volume. Phosphorus loads are from the 2018 progress scenarios in CAST (Chesapeake Bay Program, 2020), which is an estimate of

phosphorus loads under long-term average hydrology given land use and reported management as of 2018.

The Maryland Mainstem estuary volume and watershed contain approximately 31 and 44% of the total volume and watershed of the Chesapeake Bay. This ranks the Maryland Mainstem as the 2nd largest volume and 1st largest watershed area aggregated tributary in this summary (Figures 23, 24, and 25). The ratios of watershed area, nitrogen loading, and phosphorus loading to estuarine volume are consistent with other estuaries in the Chesapeake system, indicating a moderate level of susceptibility to eutrophication.

5.3 Insights on Change in the Maryland Mainstem

Completion of Section 5.3 is contingent upon stakeholder interest and availability of resources. It requires:

- *Synthesis of the information provided in previous sections and of the recent literature on explaining trends in general and any work conducted on this tributary in particular;*
- *Discussion with local technical experts to clarify insights and vet hypotheses and preliminary findings.*

6. Summary

Completion of Section 6 is contingent upon completion of Section 5.3.

References

Ator, S. W., J. D. Blomquist, J. S. Webber and J. G. Chanat, 2020. Factors driving nutrient trends in streams of the Chesapeake Bay watershed. *J. Environ. Qual.* 49:812-834, DOI: 10.1002/jeq2.20101.

Ator, S. W., J. W. Brakebill and J. D. Blomquist, 2011. Sources, fate, and transport of nitrogen and phosphorus in the Chesapeake Bay watershed: An empirical model. U.S. Geological Survey Scientific Investigations Report 2011-5167, Reston, VA, p. 27. http://pubs.usgs.gov/sir/2011/5167/.

Ator, S. W., J. M. Denver, D. E. Krantz, W. L. Newell and S. K. Martucci, 2005. A Surficial Hydrogeologic Framework for the Mid-Atlantic Coastal Plain. U.S. Geological Survey U.S. Geological Survey Professional Paper 1680. https://pubs.usgs.gov/pp/2005/pp1680/.

Ator, S. W., A. M. García, G. E. Schwarz, J. D. Blomquist and A. J. Sekellick, 2019. Toward explaining nitrogen and phosphorus trends in Chesapeake Bay tributaries, 1992–2012. *J. Am. Water Resour. Assoc.* 55:1149-1168, DOI: 10.1111/1752-1688.12756.

Bachman, L. J., B. Lindsey, J. Brakebill and D. S. Powars, 1998. Ground-water discharge and base-flow nitrate loads of nontidal streams, and their relation to a hydrogeomorphic classification of the Chesapeake Bay Watershed, middle Atlantic coast. US Geological Survey Water-Resources Investigations Report 98-4059, Baltimore, MD, p. 71. http://pubs.usgs.gov/wri/wri98-4059/.

Boynton, W. R., J. D. Hagy, J. C. Cornwell, W. M. Kemp, S. M. Greene, M. S. Owens, J. E. Baker and R. K. Larsen, 2008. Nutrient budgets and management actions in the Patuxent River Estuary, Maryland. *Estuaries Coasts* 31:623-651, DOI: 10.1007/s12237-008-9052-9.

Brakebill, J. W., S. W. Ator and G. E. Schwarz, 2010. Sources of suspended-sediment flux in streams of the Chesapeake Bay watershed: A regional application of the SPARROW Model. *J. Am. Water Resour. Assoc.* 46:757-776, DOI: 10.1111/j.1752-1688.2010.00450.x.

Bricker, S. B., J. G. Ferreira and T. Simas, 2003. An integrated methodology for assessment of estuarine trophic status. *Ecol. Model.* 169:39-60, DOI: 10.1016/s0304-3800(03)00199-6.

Bricker, S. B., B. Longstaff, W. Dennison, A. Jones, K. Boicourt, C. Wicks and J. Woerner, 2008. Effects of nutrient enrichment in the nation's estuaries: A decade of change. *Harmful Algae* 8:21-32, DOI: 10.1016/j.hal.2008.08.028.

Buchanan, C., 2020. A water quality binning method to infer phytoplankton community structure and function. *Estuaries Coasts* 43:661-679, DOI: 10.1007/s12237-020-00714-3.

Buchanan, C., R. V. Lacouture, H. G. Marshall, M. Olson and J. M. Johnson, 2005. Phytoplankton reference communities for Chesapeake Bay and its tidal tributaries. *Estuaries* 28:138-159, DOI: 10.1007/bf02732760.

Chesapeake Bay Program, 2018. Data Hub*.*

Chesapeake Bay Program, 2020. Chesapeake Assessment and Scenario Tool (CAST) Version 2019*.*

Cloern, J. E., 1982. Does the benthos control phytoplankton biomass in South San Francisco Bay? *Mar. Ecol. Prog. Ser.* 9:191-202, DOI: 10.3354/meps009191.

Eshleman, K. N., R. D. Sabo and K. M. Kline, 2013. Surface water quality is improving due to declining atmospheric N deposition. *Environ. Sci. Technol.* 47:12193-12200, DOI: 10.1021/es4028748.

Falcone, J. A., 2015. U.S. conterminous wall-to-wall anthropogenic land use trends (NWALT), 1974–2012. U.S. Geological Survey Data Series 948, Reston, VA. https://doi.org/10.3133/ds948.

Ferreira, J. G., S. B. Bricker and T. C. Simas, 2007. Application and sensitivity testing of a eutrophication assessment method on coastal systems in the United States and European Union. *J. Environ. Manage.* 82:433-445, DOI: 10.1016/j.jenvman.2006.01.003.

Fisher, T. R., E. R. Peele, J. W. Ammerman and L. W. Harding, 1992. Nutrient limitation of phytoplankton in Chesapeake Bay. *Mar. Ecol. Prog. Ser.* 82:51-63, DOI: 10.3354/meps082051.

Gellis, A. C., W. S. L. Banks, M. J. Langland and S. K. Martucci, 2005. Summary of suspended-sediment data for streams draining the Chesapeake Bay Watershed, water years 1952-2002. US Geological Survey Scientific Investigations Report 2004-5056, Reston, VA, p. 59. https://doi.org/10.3133/sir20045056.

Gellis, A. C. and G. B. Noe, 2013. Sediment source analysis in the Linganore Creek watershed, Maryland, USA, using the sediment fingerprinting approach: 2008 to 2010. *J. Soils Sed.* 13:1735-1753, DOI: 10.1007/s11368-013-0771-6.

Gellis, A. C., G. B. Noe, J. W. Clune, M. K. Myers, C. R. Hupp, E. R. Schenk and G. E. Schwarz, 2015. Sources of fine-grained sediment in the Linganore Creek watershed, Frederick and Carroll Counties, Maryland, 2008–10. U.S. Geological Survey Scientific Investigations Report 2014–5147, Reston, VA, p. 56. http://dx.doi.org/10.3133/sir20145147.

Gillespie, J. L., G. B. Noe, C. R. Hupp, A. C. Gellis and E. R. Schenk, 2018. Floodplain trapping and cycling compared to streambank erosion of sediment and nutrients in an agricultural watershed. *J. Am. Water Resour. Assoc.* 54:565-582, DOI: 10.1111/1752-1688.12624.

Gurbisz, C. and W. M. Kemp, 2014. Unexpected resurgence of a large submersed plant bed in Chesapeake Bay: Analysis of time series data. *Limnol. Oceanogr.* 59:482-494, DOI: 10.4319/lo.2014.59.2.0482.

Harding, J. L. W. and E. S. Perry, 1997. Long-term increase of phytoplankton biomass in Chesapeake Bay, 1950-1994. *Mar. Ecol. Prog. Ser.* 157:39-52, DOI: 10.3354/meps157039.

Hernandez Cordero, A. L., P. J. Tango and R. A. Batiuk, 2020. Development of a multimetric water quality indicator for tracking progress towards the achievement of Chesapeake Bay water quality standards. *Environ. Monit. Assess.* 192:94, DOI: 10.1007/s10661-019-7969-z.

Hirsch, R. M., 2012. Flux of nitrogen, phosphorus, and suspended sediment from the Susquehanna river basin to the Chesapeake Bay during Tropical Storm Lee, September 2011, as an indicator of the effects of reservoir sedimentation on water quality. U.S. Geological Survey Scientific Investigations Report 2012-5185, Reston, VA, p. 17. http://pubs.usgs.gov/sir/2012/5185/.

Hopkins, K. G., G. B. Noe, F. Franco, E. J. Pindilli, S. Gordon, M. J. Metes, P. R. Claggett, A. C. Gellis, C. R. Hupp and D. M. Hogan, 2018. A method to quantify and value floodplain sediment and nutrient retention ecosystem services. *J. Environ. Manage.* 220:65-76, DOI: 10.1016/j.jenvman.2018.05.013.

Jarvie, H. P., A. N. Sharpley, B. Spears, A. R. Buda, L. May and P. J. Kleinman, 2013. Water quality remediation faces unprecedented challenges from "legacy phosphorus". *Environ. Sci. Technol.* 47:8997-8998, DOI: 10.1021/es403160a.

Keisman, J., C. Friedrichs, R. Batiuk, J. Blomquist, J. Cornwell, C. Gallegos, S. Lyubchich, K. Moore, R. Murphy, R. Orth, L. Sanford, P. Tango, J. Testa, M. Trice and Q. Zhang, 2019. Understanding and explaining 30 years of water clarity trends in the Chesapeake Bay's tidal waters. Chesapeake Bay Program Scientific and Technical Advisory Committee STAC Publication Number 19-004, Edgewater, MD, p. 25. http://www.chesapeake.org/pubs/411_Keisman2019.pdf.

Kemp, W. M., W. R. Boynton, J. E. Adolf, D. F. Boesch, W. C. Boicourt, G. Brush, J. C. Cornwell, T. R. Fisher, P. M. Glibert, J. D. Hagy, L. W. Harding, E. D. Houde, D. G. Kimmel, W. D. Miller, R. I. E. Newell, M. R. Roman, E. M. Smith and J. C. Stevenson, 2005. Eutrophication of Chesapeake Bay: Historical trends and ecological interactions. *Mar. Ecol. Prog. Ser.* 303:1-29, DOI: 10.3354/meps303001.

King, P. B., H. M. Beikman and G. J. Edmonston, 1974. Geologic map of the United States (exclusive of Alaska and Hawaii). U.S. Geological Survey. https://doi.org/10.3133/70136641.

Kleinman, P., A. Sharpley, A. Buda, R. McDowell and A. Allen, 2011. Soil controls of phosphorus in runoff: Management barriers and opportunities. *Can. J. Soil Sci.* 91:329-338, DOI: 10.4141/cjss09106.

Langland, M. J., 2015. Sediment transport and capacity change in three reservoirs, Lower Susquehanna River Basin, Pennsylvania and Maryland, 1900-2012. U.S. Geological Survey Open-File Report 2014-1235, Reston, VA, p. 18. http://dx.doi.org/10.3133/ofr20141235.

Lyerly, C. M., A. L. H. Cordero, K. L. Foreman, S. W. Phillips and W. C. Dennison, 2014. New insights: Science-based evidence of water quality improvements, challenges, and opportunities in the Chesapeake. Annapolis, MD, p. 47. http://ian.umces.edu/pdfs/ian_report_438.pdf.

Moyer, D. L. and M. J. Langland, 2020. Nitrogen, phosphorus, and suspended-sediment loads and trends measured at the Chesapeake Bay Nontidal Network stations: Water years 1985-2018. Accessed https://doi.org/10.5066/P931M7FT.

Murphy, R. R., W. M. Kemp and W. P. Ball, 2011. Long-term trends in Chesapeake Bay seasonal hypoxia, stratification, and nutrient loading. *Estuaries Coasts* 34:1293-1309, DOI: 10.1007/s12237-011-9413-7.

Murphy, R. R., E. Perry, J. Harcum and J. Keisman, 2019. A generalized additive model approach to evaluating water quality: Chesapeake Bay case study. *Environ. Model. Software* 118:1-13, DOI: 10.1016/j.envsoft.2019.03.027.

Noe, G. B., M. J. Cashman, K. Skalak, A. Gellis, K. G. Hopkins, D. Moyer, J. Webber, A. Benthem, K. Maloney, J. Brakebill, A. Sekellick, M. Langland, Q. Zhang, G. Shenk, J. Keisman and C. Hupp, 2020. Sediment dynamics and implications for management: State of the science from long-term research in the Chesapeake Bay watershed, USA. *Wiley Interdisciplinary Reviews: Water* 7:e1454, DOI: 10.1002/wat2.1454.

Phelps, H. L., 1994. The asiatic clam (Corbicula fluminea) invasion and system-level ecological change in the Potomac River Estuary near Washington, D.C. *Estuaries* 17:614-621, DOI: 10.2307/1352409.

Pilegaard, K., 2013. Processes regulating nitric oxide emissions from soils. *Philosophical Transactions of the Royal Society B* 368:20130126, DOI: 10.1098/rstb.2013.0126.

Ruhl, H. A. and N. B. Rybicki, 2010. Long-term reductions in anthropogenic nutrients link to improvements in Chesapeake Bay habitat. *Proc. Natl. Acad. Sci. U. S. A.* 107:16566-16570, DOI: 10.1073/pnas.1003590107.

Scully, M. E., 2010. Wind modulation of dissolved oxygen in Chesapeake Bay. *Estuaries Coasts* 33:1164-1175, DOI: 10.1007/s12237-010-9319-9.

Sharpley, A., H. P. Jarvie, A. Buda, L. May, B. Spears and P. Kleinman, 2013. Phosphorus legacy: Overcoming the effects of past management practices to mitigate future water quality impairment. *J. Environ. Qual.* 42:1308-1326, DOI: 10.2134/jeq2013.03.0098.

Sharpley, A. N., 1980. The enrichment of soil phosphorus in runoff sediments. *J. Environ. Qual.* 9:521-526, DOI: 10.2134/jeq1980.00472425000900030039x.

Smith, E. M. and W. M. Kemp, 1995. Seasonal and regional variations in plankton community production and respiration for Chesapeake Bay. *Mar. Ecol. Prog. Ser.* 116:217-231, DOI.

Staver, K. W. and R. B. Brinsfield, 2001. Agriculture and water quality on the Maryland eastern shore: Where do we go from here? *Bioscience* 51:859-868, DOI: 10.1641/0006-3568(2001)051[0859:Aawqot]2.0.Co;2.

Tango, P. J. and R. A. Batiuk, 2013. Deriving Chesapeake Bay water quality standards. *J. Am. Water Resour. Assoc.* 49:1007-1024, DOI: 10.1111/jawr.12108.

Terziotti, S., 2019. Distribution of phosphorus in soils and aggregated within geologic mapping units, conterminous United States: U.S. Geological Survey data release. Accessed https://doi.org/10.5066/P918DF1E.

Testa, J. M., J. B. Clark, W. C. Dennison, E. C. Donovan, A. W. Fisher, W. Ni, M. Parker, D. Scavia, S. E. Spitzer, A. M. Waldrop, V. M. D. Vargas and G. Ziegler, 2017. Ecological forecasting and the science of hypoxia in Chesapeake Bay. *Bioscience* 67:614-626, DOI: 10.1093/biosci/bix048.

Testa, J. M. and W. M. Kemp, 2012. Hypoxia-induced shifts in nitrogen and phosphorus cycling in Chesapeake Bay. *Limnol. Oceanogr.* 57:835-850, DOI: 10.4319/lo.2012.57.3.0835.

Testa, J. M., V. Lyubchich and Q. Zhang, 2019. Patterns and trends in Secchi disk depth over three decades in the Chesapeake Bay estuarine complex. *Estuaries Coasts* 42:927-943, DOI: 10.1007/s12237-019-00547-9.

Trimble, S. W., 1975. A volumetric estimate of man-induced soil erosion on the southern Piedmont Plateau. Agricultural Research Service, U.S. Department of Agriculture Agricultural Research Service Publication ARS-S-40, pp. 142-154.

U.S. Environmental Protection Agency, 2003. Ambient water quality criteria for dissolved oxygen, water clarity and chlorophyll-a for the Chesapeake Bay and its tidal tributaries. USEPA Region III Chesapeake Bay Program Office EPA 903-R-03-002, Annapolis, Maryland.

U.S. Environmental Protection Agency, 2004. Chesapeake Bay Program analytical segmentation scheme: Revisions, decisions and rationales 1983-2003. USEPA Region III Chesapeake Bay Program Office EPA 903-R-04-008, Annapolis, Maryland, p. 64.

Wynn, T. and S. Mostaghimi, 2006. The effects of vegetation and soil type on streambank erosion, southwestern Virginia, USA. *J. Am. Water Resour. Assoc.* 42:69-82, DOI: 10.1111/j.1752-1688.2006.tb03824.x.

Zhang, Q., D. C. Brady and W. P. Ball, 2013. Long-term seasonal trends of nitrogen, phosphorus, and suspended sediment load from the non-tidal Susquehanna River Basin to Chesapeake Bay. *Sci. Total Environ.* 452-453:208-221, DOI: 10.1016/j.scitotenv.2013.02.012.

Zhang, Q., D. C. Brady, W. R. Boynton and W. P. Ball, 2015. Long-term trends of nutrients and sediment from the nontidal Chesapeake watershed: An assessment of progress by river and season. *J. Am. Water Resour. Assoc.* 51:1534-1555, DOI: 10.1111/1752-1688.12327.

Zhang, Q., T. R. Fisher, E. M. Trentacoste, C. Buchanan, A. B. Gustafson, R. Karrh, R. R. Murphy, J. Keisman, C. Wu, R. Tian, J. M. Testa and P. J. Tango, 2021. Nutrient limitation of phytoplankton in Chesapeake Bay: Development of an empirical approach for water-quality management. *Water Res.* 188:116407, DOI: 10.1016/j.watres.2020.116407.

Zhang, Q., R. M. Hirsch and W. P. Ball, 2016. Long-term changes in sediment and nutrient delivery from Conowingo Dam to Chesapeake Bay: Effects of reservoir sedimentation. *Environ. Sci. Technol.* 50:1877-1886, DOI: 10.1021/acs.est.5b04073.

Zhang, Q., R. R. Murphy, R. Tian, M. K. Forsyth, E. M. Trentacoste, J. Keisman and P. J. Tango, 2018a. Chesapeake Bay's water quality condition has been recovering: Insights from a multimetric indicator assessment of thirty years of tidal monitoring data. *Sci. Total Environ.* 637-638:1617-1625, DOI: 10.1016/j.scitotenv.2018.05.025.

Zhang, Q., P. J. Tango, R. R. Murphy, M. K. Forsyth, R. Tian, J. Keisman and E. M. Trentacoste, 2018b. Chesapeake Bay dissolved oxygen criterion attainment deficit: Three decades of temporal and spatial patterns. *Frontiers in Marine Science* 5:422, DOI: 10.3389/fmars.2018.00422.

Appendix

Additional tidal trend maps and plots are in a separate Appendix document for:

- Bottom Total Nitrogen
- Bottom Total Phosphorus
- Surface Dissolved Inorganic Nitrogen
- Surface Orthophosphate
- Surface Total Suspended Solids
- Summer Surface Dissolved Oxygen
- Surface Water Temperature